NASA CR-121025

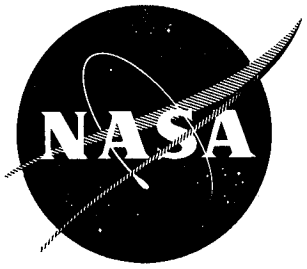


# FRACTURE AND CRACK GROWTH RESISTANCE STUDIES OF 304 STAINLESS STEEL WELDMENTS RELATING TO RETESTING OF CRYOGENIC VESSELS

*By*
*L. R. Hall and R. W. Finger*



THE BOEING COMPANY

*Prepared For*

AEROSPACE SAFETY RESEARCH AND DATA INSTITUTE
LEWIS RESEARCH CENTER
NATIONAL AERONAUTICS AND SPACE ADMINISTRATION

Contract NAS 3-12003

*Paul M. Ordin, Project Manager*

| 1. Report No. | 2. Government Accession No. | 3. Recipient's Catalog No. |
|---|---|---|
| NASA CR-121025 | | |

| 4. Title and Subtitle | 5. Report Date |
|---|---|
| Fracture and Crack Growth Resistance Studies of 304 Stainless Steel Weldments Relating to Retesting of Cryogenic Vessels | December 1972 |
| | 6. Performing Organization Code |

| 7. Author(s) | 8. Performing Organization Report No. |
|---|---|
| L. R. Hall and R. W. Finger | D180-15220-1 |
| | 10. Work Unit No. |

| 9. Performing Organization Name and Address | 11. Contract or Grant No. |
|---|---|
| The Boeing Company - Aerospace Group<br>Research and Engineering Division<br>Seattle, Washington | NAS3-12003 |
| | 13. Type of Report and Period Covered |
| | Contractor Report |

| 12. Sponsoring Agency Name and Address | 14. Sponsoring Agency Code |
|---|---|
| National Aeronautics and Space Administration<br>Lewis Research Center<br>Cleveland, Ohio | |

15. Supplementary Notes

Project Manager, Paul M. Ordin, Aerospace Safety Research and Data Institute
NASA Lewis Research Center
Cleveland, Ohio 44135

16. Abstract

This experimental program was conducted to study fracture and crack growth resistance characteristics of 304 stainless steel alloy weldments as relating to retesting of cryogenic vessels. Welding procedures were typical of those used in full scale vessel fabrication. Fracture resistance survey tests were conducted in room temperature air, liquid nitrogen and liquid hydrogen. In air, both surface-flawed and center-cracked panels containing cracks in weld metal, fusion line, heat-affected zone, or parent metal were tested. In liquid nitrogen and liquid hydrogen, tests were conducted using center-cracked panels containing weld centerline cracks. Load-unload, sustained load, and cyclic load tests were performed in air or hydrogen gas, liquid nitrogen, and liquid hydrogen using surface-flawed specimens containing weld centerline cracks. Results were used to evaluate the effectiveness of periodic proof overloads in assuring safe and reliable operation of over-the-road cryogenic dewars. It was found that proof testing alone cannot provide assurance of satisfactory structural behavior of 304 stainless steel pressure vessels. It was also shown that the application of periodic proof tests under high stress conditions is detrimental in that cyclic life is reduced.

| 17. Key Words (Suggested by Author(s)) | | 18. Distribution Statement |
|---|---|---|
| Fracture Resistance | Proof Testing | Unclassified - Unlimited |
| Fatigue Crack Growth | Pressure Vessels | |
| 304 Stainless Steel | Cryogenic | |
| Weldments | | |

| 19. Security Classif. (of this report) | 20. Security Classif. (of this page) | 21. No. of Pages | 22. Price* |
|---|---|---|---|
| Unclassified | Unclassified | | $3.00 |

* For sale by the National Technical Information Service, Springfield, Virginia 22151

# FOREWORD

This report describes an investigation of fracture and crack growth resistance studies of 304 stainless steel weldments performed by The Boeing Company from June 1970 to May 1971 under Contract NAS 3-12003. The work was administered by Mr. Paul M. Ordin of the NASA Lewis Research Center.

Boeing personnel who participated in the investigation include J. N. Masters, project leader; L. R. Hall, principal investigator; R. W. Finger, research engineer. Program support was provided by A. A. Ottlyk, non-hazardous environment testing; H. M. Olden, C. C. Mahnken and G. E. Vermilion, hazardous environment testing; C. W. Bosworth, aluminum welding; E. C. Roberts, metallurgical support; and D. G. Good, technical illustrations and art work.

The information contained in this report is also released as Boeing Document D180-15220-1.

CONTENTS

## SYMBOLS

| | |
|---|---|
| $K_I$ | Opening mode stress intensity factor |
| a | Crack depth of semi-elliptical surface flaw; one-half crack length in center cracked specimen |
| $a_i$ | Value of 'a' at beginning of test |
| $a_f$ | Value of 'a' at termination of test |
| 2c | Crack length at specimen face for semi-elliptical surface flaw |
| E | Young's modulus |
| P | Load applied to test specimen |
| R | Stress ratio, $(\text{minimum stress}/_{\text{maximum stress}})$ |
| $\phi$ | Complete elliptical integral of the second kind corresponding to the modulus $k = [(c^2 - a^2)/c^2]^{1/2}$ |
| $\sigma$ | Uniform gross tensile stress acting perpendicular to plane of crack |
| $\sigma_{ys}$ | Uniaxial tensile yield stress |
| Q | $\phi^2 - 0.212\ (\sigma/\sigma_{ys})^2$ |
| t | Gage area thickness of test specimen |
| W | Gage area width of test specimen |
| Y | Polynomial expression in terms of (a/W), used to calculate stress intensity for center cracked specimens |
| $\mu$ | Poisson's ratio |
| $M_F$ | Scalar factor used to account for effect of stress free front plate surface on stress intensity factor for surface flaws. |
| $M_K$ | Scalar factor depending on a/t and a/2c used to account for effect of stress free back plate surface on stress intensity factor for surface flaws. |

# LIST OF TABLES

## LIST OF FIGURES

## SUMMARY

This experimental program was undertaken to assess the effectiveness of periodic proof tests for providing assurance of satisfactory performance of welded 304 stainless steel pressure vessels. The experimental approach involved the testing of precracked test specimens and reflected the knowledge that crack-like defects in new structure can grow under the influence of loads and environments to a size sufficiently large to initiate failure.

Static fracture, crack growth resistance, sustained load, and cyclic load tests were conducted on 304 stainless steel weldments. Welding procedures and specimen thickness were typical of those used in full scale pressure vessels. Fracture resistance survey tests were conducted in room temperature air, liquid nitrogen and liquid hydrogen. In air, both surface-flawed and center-cracked panels containing cracks in either weld metal, fusion line, heat-affected zone, or parent metal were tested. In liquid nitrogen and liquid hydrogen, tests were conducted using center-cracked panels containing weld centerline cracks. Load-unload, sustained load, and uniform load cyclic tests were performed in air or hydrogen gas, liquid nitrogen, and liquid hydrogen using surface-flawed specimens containing weld centerline cracks. Three surface-flawed specimens containing weld centerline cracks were tested under programmed loadings in which simulated periodic proof overloads were added to a uniform cyclic load profile; in one such test, all load cycles were applied at 72F (295K) in ambient air; in the other two tests, the overloads were applied at 72F (295K) and other cycles were applied at -320F (78K).

It was observed that the 304 stainless steel annealed base metal and as-welded weld metal were very resistant to fractures originating at crack-like defects. It was concluded that it is unlikely that fractures will originate at crack-like defects during the operation of transportable cyrogenic pressure vessels. It was also shown that proof tests alone cannot provide assurance of satisfactory structural behavior of 304 stainless steel welded pressure vessels; other nondestructive inspection techniques such as X-ray and dye penetrant are required along with a proof test. Furthermore, periodic proof tests under high stress conditions were found to be detrimental in that they result in a reduction of cyclic life.

# 1.0 INTRODUCTION

Examination of vessels which have failed during test and service operations indicates that the growth of crack-like defects has been a contributing factor in numerous pressure vessel failures. Surface and embedded cracks are flaws which often go undetected in metallic pressure vessels. The flaw size required to cause fracture at a given applied gross stress is called the critical size. Catastrophic failure can be expected during testing if the vessel contains an initial flaw which exceeds the critical size at the proof stress level. Failure during service will occur when the initial flaw is less than critical size at the proof stress, but grows until it reaches the critical size at the operating stress level. On the other hand, only leakage occurs in the pressure vessel when the initial flaw grows through the thickness of the wall prior to reaching the critical size. As a result, considerable effort is being directed to characterization of crack growth in metallic alloys. Most investigations have used macroscopic experimental observations to investigate the phenomenology of crack growth. Such observations have shown that crack growth behavior can be related to the stress intensity factor that is defined by modified linear elastic fracture mechanics theory.

Pressure vessel design methods have been developed (1)* for assuring that crack-like defects will not grow sufficiently to initiate failure during the operational life of pressure vessels. Present design methods are most effective when applied to pressure vessels in which critical flaw sizes at proof stress levels are less than the thickness of the vessel wall. The methods become decreasingly effective as fracture toughness increases and/or thickness decreases. The approach is based on interpretation of results of a successful proof test combined with subcritical crack growth data obtained from tests of precracked laboratory specimens. Test data are correlated and related to full size structure behavior using modified linear elastic fracture mechanics parameters.

*Numbers in parentheses refer to references at end of report.

This program was undertaken to evaluate the effectiveness of periodic proof pressure testing for providing assurance of satisfactory performance of welded pressure vessels fabricated from 304 annealed stainless steel plate. Static fracture, crack growth resistance, sustained load, and cyclic load tests were conducted on precracked 304 stainless steel weldments. Welding procedures and specimen thickness were typical of those used in full scale pressure vessels. Fracture resistance survey tests were conducted in air, liquid nitrogen and liquid hydrogen. In air, both surface flawed and center-cracked panels containing cracks in either weld metal, fusion line, heat affected zone, or parent metal were tested; surface flawed specimens were loaded to failure and loads at which the cracks penetrated the specimen thickness and at which failure occurred were measured; center-cracked panels were incrementally loaded to ninety-five percent of the weld metal yield stress and the amount of crack growth that occurred during each load increment was observed. Load-unload, sustained load, and cyclic load tests were conducted in air or hydrogen gas, liquid nitrogen, and liquid hydrogen using surface-flawed specimens containing weld centerline cracks. The load-unload and sustained load tests were undertaken to evaluate the amount of crack growth that could be induced by a typical proof overload. Cyclic load tests were performed by subjecting specimens to uniform stress cycling after a single proof overload. Finally, three surface-flawed specimens containing weld centerline cracks were tested under programmed loadings in which periodic proof overloads were added to a uniform cyclic load profile; in one programmed load test, all load cycles applied at 72F (295K) in ambient air; in the other two tests, the overloads were applied at 72F (295K) and other cycles were applied at -320F (78K).

The remainder of this report contains five sections. Section 2 includes a brief background description of the use of stress intensity factors to correlate and apply crack growth and fracture data obtained from test of precracked spcimens. Section 3 presents details of the test program. Section 4 describes materials and procedures. Sections 5 and 6 present results and discussions, and observations, conclusions, and recommendations, respectively. In the body of this report, the primary system of units is the

foot-pound-second (FPS) system. However, all numerical quantities are also given in international system (SI) units in parentheses after the FPS units. Both systems of units are used on all figures but tables contain only FPS units. Multipliers for converting FPS to SI units are included in the appendix.

## 2.0 BACKGROUND

The surface flaw is a realistic model of failure origins in pressure vessels. Hence, surface-flawed specimens are tested extensively to develop design data for fracture control methods used within the aerospace industry. In this program, developments used in the aerospace industry have been applied to investigations of structural integrity of transportable cryogenic vessels. Most surface-flawed specimen data have been correlated and applied using the opening mode stress intensity factor defined by linear elastic fracture mechanics theory (1). In this program, specimens were designed to model potential failure origins so that the test data would be directly representative of full size vessel behavior. As a result, all conditions required for the application of the stress intensity factor approach were not met in these tests. The stress intensity factor approach was used to relate specimen and full scale dewar behavior and will be discussed briefly in the following paragraphs.

The characteristic feature of all linear elastic solutions for stresses in the neighborhood of cracks in homogeneous isotropic materials is that the stress fields in the immediate vicinity of any crack tip are identical if the stress intensity factors are equal. Consequently, the extension of two different cracks proceeds under the influence of similar stress environment as long as the stress intensity factors are equal and inelastic behavior is of no major influence.

A large body of experimental evidence has shown that, for given material and temperature, there is a critical value of stress intensity factor at which a crack becomes unstable and propagates very rapidly. The critical stress intensity factor value is considered to be a material property called fracture toughness. It has also been shown that at stress intensity factors less than the critical value, the growth rate of cracks under both cyclic and invariant loading is related to stress intensity factor (2).

### Stress Intensity Factors

Relationships between stress intensity factor, crack dimensions, body dimensions, and nominal stress field have been developed for a number of cracked bodies.

In this program, both center cracked and surface flawed specimens were tested. For center cracked specimens (Figure 1), opening mode stress intensity factors ($K_I$) are given by the expression (3)

$$K_I = Y\sigma \sqrt{a} \tag{1}$$

where values of Y and definition of symbols are included in Figure 1. For semi-elliptical surface flaws (Figure 2), a number of stress intensity factor solutions involving varying degrees of approximations exist (4). The maximum value of stress intensity factor occurs at the point of deepest penetration of the flaw designated by Point A in Figure 2 and is usually expressed as

$$K_I = M_F M_K \sigma \sqrt{\frac{\pi a}{Q}} \tag{2}$$

where $M_F$ and $M_K$ are factors that account for effects of the front and back plate surfaces. Variables are defined in Figure 2 and in the list of symbols (page iv). A discussion of the various solutions for $M_F$ and $M_K$ can be found in Reference 4.

## 3.0 TEST PROGRAM

The test program for investigating fracture and subcritical crack growth characteristics of 304 stainless steel weldments is summarized in Table 1. Fracture resistance survey tests were conducted to evaluate the relative resistance to fracture of weld metal, fusion line, heat affected zone, and parent metal (see Figure 3). Both center cracked (CC) and surface flawed (SF) specimens were tested in air at 72F (295K), $LN_2$ at -320F (78K), and $LH_2$ at -423F (20K). The remaining load-unload, sustained load, and cyclic load tests were performed in air at 72F (295K) or hydrogen gas at 40 to 60F (278-288K), liquid nitrogen, and liquid hydrogen, using SF specimens containing weld centerline surface cracks. Load-unload and sustained load tests were conducted to evaluate the effect of both proof overloads and hydrogen gas on surface flaw growth in weld metal. All such tests were conducted using peak stress levels equal to 95 percent of the measured weld metal tensile yield stress. Cyclic load tests were undertaken to evaluate the effect of cyclic loadings on crack growth after a proof overload; specimens were first subjected to a static loading to 95 percent of the weld metal tensile yield stress, and were then subjected to uniform sinusoidal fatigue loadings having a peak stress of 63 percent of the weld metal yield stress. The stress levels used in these tests are higher than nominal membrane stress levels in full size vessels and are representative of areas subjected to higher than nominal stresses due to causes such as out-of-contour geometry.

Three programmed load tests were conducted to evaluate the effects of periodic proof overloads on the fatigue crack growth behavior of 304 stainless steel as-welded weld metal. The specimens were repeatedly subjected to an arbitrarily selected block of 31 sinusoidal zero-to-tension loading cycles until the surface cracks penetrated the specimen thickness. The loading block consisted of one cycle having a peak stress of 45 ksi (310.3MN/$m^2$) followed by 30 cycles having a peak stress of 30 ksi (206.9 MN/$m^2$). In one test, all cycles were applied at 72F (295K). In the other two tests, the overload cycle was applied at 72F (295K) and the lower stress cycles were applied at -320F (78K).

# 4.0 MATERIALS AND PROCEDURES

## 4.1 Materials

AISI 304 stainless steel plate material was used in the fabrication of all specimens. The plate material, 0.375 by 48 by 96 inches (0.95 by 122 by 244 cm) was purchased in the annealed condition per MIL-S-5059C. Typical mechanical properties for this material (5) are: ultimate tensile strength $\sim$ 85 ksi (586 $MN/m^2$); tensile yield strength $\sim$ 30 ksi (207 $MN/m^2$); elongation in 2 inches (5.08 cm) gage length $\sim$ 60 percent; reduction in area $\sim$ 70 percent. Specification limits on chemical composition are listed in Table 2. AISI 308 stainless steel weld wire was used for welding. Both spooled 1/16 inch (1.6 mm) diameter and 36 inch (91.4 cm) straight lengths of 3/32 inch (2.38 mm) diameter wire were purchased per MIL-T-5031B, Class I. Specification limits on chemical composition are listed in Table 2.

Mechanical property data generated by The Boeing Company for both annealed 304 stainless steel plate material and as-welded welds are listed in Table 3 and plotted against temperature in Figure 4. All properties were typical except the yield strength of the plate material which was higher than typical. Values of weld metal tensile yield stress used in calculating loads for welded test specimens were 47 ksi (324 $MN/m^2$) at 72F (295K), 58 ksi (400 $MN/m^2$ at -320F (78K), and 68 ksi (469 $MN/m^2$) at -423F (20K). These values are averages of the two data points listed in Table 3 for -320F (78K) and -423F (20K). At 72F (295K), a value of 47 ksi (324 $MN/m^2$) was used because the planned peak test stress of ninety-five percent of the tensile yield stress would have been greater than the smaller measured yield stress when based on the average of the two measured values.

## 4.2 Procedures

### 4.2.1 Welding

Weld panels, 0.375 by 48 by 48 inches (0.95 by 122 by 122 cm) for center-cracked specimens and 0.375 by 27 by 48 inches (0.95 by 69 by 122 cm) for SF specimens, were prepared by joining two identical panel halves. Edge

preparation consisted of a single-V configuration with a 60 degree included angle, 0.065 inch (0.17 cm) deep land, and 0.10 inch (0.25 cm) root opening. The joint was wiped clean with methyl ethyl ketone solvent (MEK) immediately prior to welding. Panels were welded using a three pass procedure. A single manual GTA pass was used to close the root gap and two manual GMA passes were deposited from the opposite side to complete the weld. A power driven stainless steel bristle brush was used to clean each weld bead. Further details of the welding procedure are given below.

| Pass Number | Location | Welding Process | Wire Type | Wire Dia.-in(cm) | Current (amps) | Voltage (Volts) |
|---|---|---|---|---|---|---|
| 1 | Bottom | Manual GTA | AISI 308 Rod | 3/32 (0.24) | 125 | 15 |
| 2 | Top | Manual GMA | AISI 308 Wire | 1/16 (0.16) | 230-240 | 25 |
| 3 | Top | Manual GMA | AISI 308 Wire | 1/16 (0.16) | 240-250 | 30 |

NOTE: Gas coverage was pure Argon at 15 CFH (0.42 $m^3$/hr)

A Vicar 300-amp power supply was used for the GTA welding, and a Linde SVI-500 power supply was used for the two GMA passes.

All panels were X-rayed after welding. The radiographs revealed porosity in all panels. Those areas containing excessive porosity were discarded when cutting specimens from the weld panels.

### 4.2.2 Specimen Preparation

All testing was accomplished using one surface-flawed (SF), one center cracked (CC), and one mechanical property specimen configuration as detailed in Figures 5, 6, and 7, respectively. The surfaces of all specimens containing welds were machined just enough to clean up the weld bead. Grip holes were drilled to a tolerance of $\pm$ 0.001 inch (0.025 mm).

All SF specimens were precracked by growing fatigue cracks from starter slots machined with an electrical discharge machine (EDM), circular electrodes, and kerosene dielectric. The tips of the 0.06 inch (1.5 mm) thick electrodes were

machined to a radius of 0.003 inch (0.076 mm) and an included angle of twenty degrees. The EDM slot and surrounding area were brushed clean with commercial grade naphtha and blown dry with compressed air. Fatigue cracks were then grown at 72F (295K) using sinusoidal tension-tension fatigue cycles with an R value ($\frac{\sigma min}{\sigma max}$) of 0.06, and a frequency of 1800 cpm (30 Hz). Several different peak cyclic stress levels were used to grow the cracks. The maximum cyclic stresses used for all but two specimens having flaw depths of 0.15, 0.23, and 0.30 inch (3.8, 5.8 and 7.6 mm) were 25, 20 and 20 ksi (172, 138 and 138 $MN/m^2$, respectively. Specimens 10-4 and 11-1 were fatigue cracked using peak cyclic stress levels of 30 and 25 ksi (207 and 172 $MN/m^2$), respectively. The maximum cyclic stress used for all but two specimens having initial flaw depths of 0.07 inch (1.78 mm) was 35 ksi (241 $MN/m^2$). The two exceptions were specimens 9-1 and 9-2 in which fatigue cracks were initiated using peak cyclic stress levels of 50 and 45 ksi (345 and 310 $MN/m^2$), and were grown under stress levels of 40 and 35 ksi (276 and 241 $MN/m^2$, respectively. The maximum stress level during the first loading cycle in all SF specimen tests was greater than the precracking stress. Hence, variations in precracking stress are believed to have no measurable effect on test results.

Center cracked specimens were also precracked by growing fatigue cracks from starter slots. Sharp tips having a root radius of 0.003 inch (0.076 mm) and a 60 degree included angle were machined at the end of 0.125 inch (0.317 cm) wide starter slots using an electrical discharge machine. Fatigue cracks were grown to a length of about 0.5 inch (1.3 cm) under a peak gross area cyclic stress of 10 ksi (69 $MN/m^2$).

### 4.2.3 Testing

All tests except those in gaseous hydrogen were conducted at either 72F (295K), -320F (78K) or -423F (20K). Tests at 72F (295K) were performed within an enclosed air conditioned laboratory. Specimens were stored in the laboratory for several days prior to testing. Tests at -320F (78K) and -423F (20K) were conducted by submerging specimens in $LN_2$ or $LH_2$, respectively. Specimens were soaked for 15 minutes prior to load application. Tests in $GH_2$ were conducted at ambient outdoor temperatures ranging from 40 to 60F (278 to 288K).

Fracture Resistance Tests - Surface-flawed and center-cracked panels were prepared with cracks located in the various weldment zones. Specimen surfaces were etched lightly to locate the weld bead. A hardness survey taken across the weld, HAZ, and base metal revealed no hardened area. Cracks were located at the weld centerline, as near as possible to the fusion line, and in the parent metal one inch away from and parallel to the weld centerline.

Surface-flawed specimens were loaded to failure in room air at a loading rate of 100 kips/minute (7.4 kN/sec). Specimens were instrumented with pressure cups located on both the front and back specimen faces at the center of the specimen. The pressure cups were similar in design to those pictured in Figure 8. The cups were sealed with teflon O-rings and were clamped to the specimen. The cup on the flawed surface was pressurized to 10 psig (6.9 $kN/m^2$) with welding grade argon gas. Pressure in both front and back cups was continuously monitored throughout the test. When the cracks penetrated the specimen thickness, abrupt changes in pressure were observed in both cups.

Center-cracked panels were tested at 72°F (295K) in room air, at -320F (78K) in $LN_2$, and at -423F (20K) in liquid hydrogen. Specimens were instrumented with clip gages spring loaded against knife edges machined into the specimen at the center of the crack as shown in Figure 9. The gages were used to continuously measure the opening mode crack displacement at the center of the crack as a function of applied load. For the 72F (295K) tests, specimens were incrementally loaded to average stresses on the net section (specimen width minus crack length times thickness) of 50, 75, 95 and 105 percent of the uniaxial weld metal yield stress of 47 ksi (324 $MN/m^2$). The specimens were held at each load until crack displacement had stabilized. The flaw tip was then closely examined under load by means of a specially designed microscope to determine whether any flaw growth had occurred during the prior load history. For -320F (78K) and -423F (20K) tests, specimens were loaded to average stresses on the net section of 95 percent of the corresponding weld metal yield stresses (58 ksi (400 $MN/m^2$) and 68 ksi (469 $MN/m^2$), respectively). The load was maintained until crack displacement had stabilized. All specimens were then subjected to fatigue loadings at room temperature to delineate the flaw periphery, and loaded to failure.

Load-Unload Tests - Load-unload tests were conducted by loading surface flawed specimens to a stress level of 95 percent of the weld metal yield stress at a rate of 50 kips/minute (3.7 kN/sec), and then immediately unloading the specimens. Time at maximum load was less than one second. All specimens were subsequently subjected to fatigue and static failure loadings at room temperature to delineate and reveal any flaw growth that occurred during the load-unload sequence.

Sustained Load Tests - Sustained load tests were conducted in argon and hydrogen gases, $LN_2$ and $LH_2$. Gaseous environments were contained in pressure cups surrounding the flaw. Gage areas of test specimens were completely submerged in liquid environments. Selected specimens were instrumented with clip gages spring loaded against integrally machined knife edges at the mouth of the surface flaw. Continuous recordings of crack displacement versus load were obtained using X-Y recorders. After the sustained load test, all specimens were subjected to fatigue and static failure loadings at room temperature to delineate and reveal any flaw growth that occurred during the sustained load test.

Cyclic Load Tests - All specimens were subjected to an overload having a peak stress equal to 95 percent of the appropriate weld metal yield stress prior to fatigue testing. The overload was applied at a rate of 50 kips/minute (3.7 kN/sec) and was rapidly decreased to zero as soon as peak load was reached. After the overload, specimens were subjected to uniform sinusoidal fatigue cycles having a peak stress of 63 percent of the appropriate weld metal yield stress, a stress ratio, R, of zero and frequency of 25 cpm (0.42 Hz) at 72F (295K) and -320F (78K), and a stress ratio of 0.1 and frequency of 2.5 cpm (0.042 Hz) at -423F (20K). Frequency and R value were different at -423F (20K) due to limitations imposed by the test equipment. Specimens containing the largest flaws were cycled until the flaw penetrated the specimen thickness. Flaw breakthrough for 72F (295K) and -320F (78K) was detected by monitoring the pressure in a cup containing 10 psig (6.9 $kN/m^2$) helium gas located on the back specimen face directly opposite the flaw location. Successive pressure drops that occurred during each cycle after the flaw penetrated the specimen thickness were distinctly visible on the pressure versus cycles readout. At -423F

(20K), pressure cups were used on both specimen faces in order to circumvent sealing problems due to the use of helium gas at low temperatures. The cup on the flawed face was pressurized with a continuous supply of helium gas from a pressurized bottle. The cup on the back face was left unpressurized. A record of the pressure in the rear surface cup included in Figure 10 shows that the loading cycle during which flaw breakthrough occurred is clearly defined.

Programmed Cyclic Tests - Specimens were subjected to periodic proof overload tests consisting of one cycle having a peak stress of 95 percent of the weld metal stress (45 ksi, 310.3 $MN/m^2$) followed by 30 cycles having a peak stress of 63 percent of the weld metal stress (30 ksi, 206.9 $MN/m^2$). Test procedures were identical to those for the cyclic tests. In one test, all cycles were applied at 72°F (295K) and in the other two tests, the overload stress was applied at 72°F (295K) and the lower stress cycles at -320F (78K).

Mechanical Property Tests - Mechanical properties were measured using the specimen configuration in Figure 7. Specimens were loaded at a strain rate of 0.005/minute until the yield strength had been exceeded. The strain rate was then increased to 0.02/minute until failure.

# 5.0 RESULTS AND DISCUSSION

## 5.1 Fracture Resistance Survey Tests

Results of the fracture resistance survey SF specimen tests are included in Table 4. It was attempted to locate flaw tips at the weld centerline, fusion line, heat affected zone, and parent metal. An examination of the failed specimens showed that the tips of flaws intended for the fusion line and heat affected zone were actually located in weld metal adjacent to the fusion line. Failure stresses for all specimens were nearly equal and the flaw penetrated the specimen thickness at or near the failure stress.

Results of fracture resistance center-cracked panel tests are included in Table 5. Specimens tested at 72F (295K) were incrementally loaded to average stress levels on the net section equal to 50, 75, 95 and 105 percent of the weld metal tensile yield stress. Crack lengths at the beginning and end of each test are listed in the table. A typical record of load versus crack displacement measured at the center of the specimen is reconstructed in Figure 11. After the application of each load increment, the load was held constant until crack displacement stabilized. Crack displacement continued to increase for about ten minutes after the attainment of each targeted load. After crack displacement stabilized, visual inspection of the crack tip with a microscope revealed noticeable crack tip blunting but no crack growth was observed in any of the specimens.

An examination of the fracture surfaces showed that crack growth had occurred in specimen CC-3 which contained a weld centerline crack. The crack length increased from 11.93 to 12.35 inches (30.30 to 31.37 cm) at the mid plane of the specimen, but no crack growth occurred at the specimen surfaces. No crack growth was observed in any other specimens.

Results of center cracked panel tests conducted at -320F (78K) and -423F (20K) are also included in Table 5. Both -320F (78K) specimens and one -423F (20K) specimen (CC-7) were loaded to a net section stress level of 95 percent of the corresponding weld metal tensile yield stress. The load was sustained for 15 minutes until crack displacements had stabilized, and was then reduced to zero.

Load versus crack displacement records obtained for -320F (78K) specimen CC-4 and -423F (20K) specimen CC-7 are included in Figures 12 and 13, respectively. Small amounts of crack growth were noted on the fracture surfaces of specimens CC-6 and CC-7 as indicated in Table 5. The other -423F (20K) specimen (CC-8) failed just before the targeted stress level was reached. The load versus crack displacement record for specimen CC-8 is included in Figure 13.

Records of load versus crack displacement for the 72F (295K) center cracked panels were highly nonlinear even though little or no crack extension occurred. This result indicates that crack tips are able to withstand considerable plastic flow at 72F (295K) while undergoing little or no crack growth.

Results of the center cracked panel tests were used to estimate crack lengths below which failure would not be expected to occur in full size dewars. Since none of the 72F (295K) and -320F (78K) test panels failed under maximum applied net section stress levels of 95 percent of the weld metal yield stress, the critical stress intensity factors are larger than the values existent at the crack tips under the maximum applied loads. At -423F (20K), one panel failed at an applied stress of 0.95 $\sigma_{ys}$ and this result was used to calculate a critical stress intensity factor. Stress intensity factors for test panels were calculated from the equation.

$$K_p = 2.1\ \sigma\sqrt{\pi a} \qquad \text{(Ref 3)}$$

where $K_p$ is stress intensity factor, $\sigma$ is applied gross stress, and 'a' is half crack length (3). In areas of uniform membrane stress, full scale dewar behavior is nearly equivalent to that of an infinitely wide flat plate (6) and so corresponding crack lengths for dewars were calculated from the equation

$$2a_d = (2\pi)(K_p/\sigma)^2$$

where $2a_d$ is minimum critical crack length for the dewar welds, and $\sigma$ is applied gross stress. Results of calculations for $\sigma$ = 47 ksi (324 MN/m$^2$) (assumed proof stress) and $\sigma$ = 31 ksi (214 MN/m$^2$) (assumed working stress) are included in the last two columns of Table 5.

The minimum critical crack lengths at the assumed proof test stress level appear to be greater than crack lengths that would be expected to result in detectable leaks at operating stress levels. Hence, it is unlikely that undetected through-the-thickness cracks would cause proof test failures of full scle dewars. Minimum critical crack lengths at the assumed operating stress level are very long and leaks should be detected at crack lengths significantly less than the critical value.

## 5.2 Load-Unload Tests

Two series of tests were undertaken to determine if proof overloads could initiate failure or crack growth at embedded crack-like defects in 0.375 inch (0.95 cm) thick 304 stainless steel welds. In the first test series, load-unload tests were conducted by loading specimens to 95 percent of the weld metal tensile yield stress followed immediately by rapid unloading.

Specimen dimensions, test conditions, and results for the load-unload tests are included in Table 6. Four specimens containing weld centerline surface cracks were tested in each of three environments including room temperature air, $LH_2$, and $LN_2$. One nominal flaw depth-to-length ratio (a/2c = 0.15) and four flaw depth-to-thickness ratios (a/t = 0.2, 0.4, 0.6, 0.8) were investigated in each environment. Minor amounts of crack growth were noted at the peripheries of the two largest flaws tested in room temperature air and $LN_2$. All other tests produced no failures nor observable crack growth.

## 5.3 Sustained Load Tests

In the second test series, sustained load tests were performed in potential proof test fluids and in $GH_2$ at applied stress levels of 95 percent of the weld metal tensile yield stress. Sustained-load test data are included in Table 7. Specimens containing weld centerline surface cracks were tested in air and hydrogen gas at 72F (295K), $LN_2$ and $LH_2$. One nominal a/2c ratio (0.15) and one nominal a/t ratio (0.75) was used, in all tests. Test durations were either 5 or 20 hours except for one $LN_2$ specimen that was tested for 15.7 hours. Crack growth was noted in all tests. The appearance of the fracture surfaces is illustrated by the photograph of the fracture face of specimen 14-1 in Figure 14.

Specimens used for 20 hour tests were instrumented with clip gages to continuously monitor maximum relative opening mode crack surface displacement at the center of the crack. The resulting crack displacement versus time records are shown in Figure 15. Increases in crack surface displacement during the test runs were inversely proportional to test temperature. At all temperatures, the rate of increase of displacement diminished throughout each test and appeared to reach zero after 20 hours at room temperature and 10 hours at cryogenic temperatures.

The test records in Figure 15 bear a strong resemblance to the initial portion of creep curves and to the early stages of crack length versus time curves obtained from sustained load tests of AM350 steel center-cracked specimens in purified argon gas (7). Consequently, it was concluded that the crack growth observed in these sustained load tests was probably not environmentally assisted but was due to mechanical processes. On the other hand, more crack growth was observed for tests in $GH_2$ than for identical tests in gaseous argon (see Table 7). This observation makes it unwise to conclude on the basis of these tests that 304 stainless steel welds are immune to hydrogen assisted slow crack growth.

The foregoing results indicate that proof tests of full scale cryogenic dewars can induce small amounts of crack growth in the presence of large crack-like defects. It is estimated that proof tests conducted in less than 30 minutes will result in less than 0.01 inch (0.25 mm) of crack growth.

## 5.4 Cyclic Tests

Results of cyclic tests are included in Table 8. At least four specimens were cycled in each of three environments including air, $LN_2$ and $LH_2$. One initial flaw depth-to-length ratio ($a/2c \simeq 0.15$) and four initial flaw depth-to-thickness ratios ($a/t = 0.2, 0.4, 0.6, 0.8$) were tested in each environment. The loading profile for each environment consisted of a single load having a peak stress of 95 percent of the weld metal tensile yield stress, followed immediately by uniform sinusoidal loading cycles having a peak stress of 63 percent of the weld metal yield stress. With one exception, specimens fabricated with initial a/t values of 0.6 and 0.8 were cycled until the surface crack barely penetrated the specimen thickness. The number of

loading cycles required to accomplish this result are listed in Table 8. The one exception was specimen 5-3 which was tested at -423F (20K).

The fracture face of specimen 13-1 included in Figure 14 shows a flaw that has barely penetrated the specimen thickness. Specimens fabricated with initial a/t values of 0.2 and 0.4 were subjected to 10,000 loading cycles in air and $LN_2$, and 2250 cycles in $LH_2$. Flaw dimensions both before and after the application of the 10,000 or 2250 loading cycles are listed in Table 8.

Results of the cyclic tests are plotted in Figure 16 on semi-log plots of net thickness (distance between crack tip and back specimen face $(t-a_i)$ versus cycles, where t is specimen thickness, and '$a_i$' is initial flaw depth. Since flaw depth was the only variable in these tests, the cyclic data should fall very close to a single curve on such a plot. For each specimen that was cycled until the flaw penetrated the specimen thickness, the number of loading cycles required to accomplish this result is plotted against the net thickness existent at the outset of the test $(t-a_i)$. For specimens in which the flaw was not grown through the specimen thickness, two data points are plotted representing conditions at the outset and termination of each test. The ordinates of the two points are $(t-a_i)$ and $(t-a_f)$ where $a_i$ and $a_f$ are flaw depth at the beginning and termination of the test. The abscissas of the two points ($x_1$ and $x_2$) must satisfy the relationship $x_1 - x_2 = \log N_o$ where $N_o$ is the number of cycles required to grow the flaw depth from $a_i$ to $a_f$ (10,000 or 2250) cycles in these tests). The values of $x_1$ and $x_2$ were chosen so that $x_1 - x_2 = \log N_o$ and so the data from all the tests could be represented by a single curve. Further background concerning this method of data presentation can be found in Reference 1. At -423F (20K), specimen thickness varied slightly since the surface of instrumented specimens had to be machined to effect a good sealing surface. Since thickness was varied by only about 5 percent, the use of a single curve to represent the data is still a reasonable approach to data evaluation.

## 5.5 Programmed Load Tests

Three programmed load tests were conducted to evaluate the effects of periodic proof overloads on the fatigue crack growth behavior of 304 stainless steel as-welded weld metal. Test procedures were identical to those for the

previously described 72F (295K) and -320F (78K) cyclic tests except for specimen thickness and load/temperature histories. Specimen gage areas were machined flat and parallel in order to provide a suitable surface finish for mounting and sealing pressure cups used to detect crack breakthough. The resulting specimen thickness was 0.36 inch (0.65 cm). All specimens were repeatedly subjected to a block of 31 sinusoidal zero-to-tension loading cycles until the surface cracks penetrated the specimen thickness. The loading block consisted of one cycle having a peak stress of 45 ksi (310.3 $MN/m^2$) followed by 30 cycles having a peak stress of 30 ksi (206.9 $MN/m^2$). In the first test, all cycles were applied at 72F (295K). In the other two tests, the 45 ksi (310.3 $MN/m^2$) cycle was applied at 72F (295K) and the subsequent cycles at 30 ksi (206.9 $MN/m^2$) were applied with the specimen at -320F (78K). For the latter two tests, specimen temperature was monitored using a thermocouple located on the specimen centerline 0.1 inch (0.25 cm) away from the plane of the crack. The cracks were subjected to a welding grade helium gas environment throughout each test using the crack breakthrough detection instrumentation shown in Figure 8.

Test results and details are summarized in Table 9 and Figure 17. In Figure 17, the number of loading cycles required to grow the crack until the crack depth barely penetrated the specimen thickness is plotted against the depth of ligament between the crack tip and back specimen face at the outset of each test. A scatter band including 72F (295K) and -320F (78K) cyclic data from Figure 16 is shown in the same figure. The scatter band includes data from specimens that were subjected to a single 45 ksi (310.3 $MN/m^2$) overload at the outset of the test followed by cycling under uniform zero-to-tension cycles with a peak stress of 30 ksi (206.9 $MN/m^2$). Figure 17 shows that the data resulting from all three programmed load tests were in good agreement and that the application of periodic overloads reduced the number of loading cycles to crack breakthrough. The good agreement was anticipated due to the prior cyclic test results (Section 5.4) which yielded very little effect of temperature on fatigue crack growth rates in the 304 stainless steel welds at temperature ranging from 72F (295K) to -320F (78K).

Crack breakthrough did not always occur during an overload cycle. In the test conducted entirely at room temperature, the crack penetrated the specimen thickness during the eighteenth 30 ksi (206.9 $MN/m^2$) cycle after the application of the last proof overload. After the crack penetrated the specimen thickness, the application of overloads was discontinued and the specimen was cycled to failure using 30 ksi (206.9 $MN/m^2$) stress cycles. The specimen failed after a total of 24,557 cycles at which time the crack had grown to a length of 4.8 inches (12.2 cm). The net section stress at failure was 83 ksi (572 $MN/m^2$) which is the ultimate strength of the weld metal. In one test conducted with overloads applied at 72F (295K) and subsequent cycling at -320F (78K), the crack penetrated the specimen thickness during an overload; in the other such test, it was not clear whether crack breakthrough occurred during the overload or three cycles thereafter. <u>These results make it clear that proof testing cannot be used to guarantee minimum fatigue performance capabilities of 304 stainless steel welds</u>.

The reduced cyclic life in the programmed load tests was undoubtedly due to the effect of the periodic overloads. It was not clear prior to the tests whether the periodic overload would be beneficial or detrimental. Since overloads are known to retard crack growth in some materials during subsequent lower stress cycles, it was hoped that the overloads for 304 stainless steel weld metal would have an overall beneficial effect by increasing the total number of loading cycles required to grow the crack through the specimen thickness. However, it is evident that the crack growth induced by the overloads more than offset any retarding effect. It is believed that the reduction in life due to the periodic overloads was accentuated by high fatigue crack growth rates during the overloads as a result of the material. It is known (8) that fatigue crack growth rates at fixed stress intensity levels can increase when peak cyclic stress levels approach the yield stress of the material containing the crack. Since peak cyclic stress levels during the overloads were equal to ninety-five percent of the weld metal yield stress, it is reasonable to conclude that crack growth during overloads was accelerated by the high stress levels.

The foregoing tests are considered to be representative of areas in cryogenic dewars that are subjected to stress levels that approach the yield stress during proof testing. Nominal membrane stress levels in full scale dewars should be less than the stress levels used in these tests. However, it is possible that areas containing fittings or out-of-contour conditions would be repeatedly subjected to proof stress levels higher than nominal values. The tests conducted herein are thought to be representative of the most detrimental effects on fatigue crack growth generated by periodic proof loadings of full-scale cryogenic dewars.

## 5.6 Static Fracture Tests

Results of a number of static fracture tests of SF specimens containing weld centerline surface cracks are included in Table 10 and Figure 18. These results were obtained from fracture tests of specimens that had been previously tested under load-unload, sustained load, or cyclic load profiles, then subjected to low stress fatigue loadings to delineate the flaw growth that occurred during the prior tests. Results for two specimens containing flaws that had barely penetrated the specimen thickness are plotted at $a/t = 1.0$. Flaw depth-to-length ratios for all specimens ranged between 0.15 and 0.22. These data show that surface cracks with a/2c greater than about 0.2 would not be expected to initiate a catastropic rupture at stress levels less than about 49 ksi (338 $MN/m^2$).

# 6.0 OBSERVATIONS, CONCLUSIONS, AND RECOMMENDATIONS

## Observations and Conclusions

The 304 stainless steel annealed base metal and as-welded metal were very resistant to fracture initiating at crack-like defects. For the 0.375 inch (0.95 cm) thick welds tested in this program, surface cracks having depth by length dimensions of approximately 0.29 x 2.0 inches (0.71 x 5.1 cm) did not originate fractures when subjected to uniaxial stress levels equal to ninety-five percent of the yield stress of the weld metal at temperatures ranging from +70 to -423F (295 to 20K).

Using test data for center cracked panels and linear elastic fracture mechanics theory, it was estimated that critical crack lengths for through-the-thickness cracks at weld centerlines in full scale dewars are in excess of four inches (10 cm) at temperatures ranging from +70 to -423F (295 to 20K), and for a uniform gross tensile stress level equal to 47 ksi (324 $MN/m^2$). This stress level is believed to be greater than nominal membrane stress levels generated by typical proof pressure tests of full scale dewars. Similar calculations yielded critical crack lengths in excess of nine inches (23 cm) at a uniform stress level of 31 ksi (214 $MN/m^2$); this stress level is also thought to be greater than nominal membrane stresses induced by working pressures in full scale dewars.

It is unlikely that fractures will originate at crack-like defects during the operation of over-the-road transportable cryogenic dewars fabricated from 304 stainless steel. One possible source of fracture is a long embedded defect that goes undiscovered prior to a proof test. If the defect length is greater than the critical through crack length at the peak proof pressure, it could initiate a fast running crack during the proof test. It is unlikely that crack-like defects that pass a proof test will grow sufficiently during subsequent operation and originate a fast running crack before penetrating the tank wall thickness and creating a detectable leak.

A single proof overload was found to induce only small amounts of crack growth at surface cracked 304 stainless steel weld centerlines. The proof overload

consisted of a uniaxial stressing to ninety-five percent of the weld metal yield stress. It was estimated that a proof test of full scale dewars that is performed in less than thirty minutes will result in less than 0.01 inch (0.25 mm) of crack growth in the presence of large crack-like defects in the membrane areas of the dewars. However, it was found that periodic proof testing to the same stress level every 31st cycle did reduce the remaining cyclic life.

It was shown that proof tests alone cannot provide assurance of satisfactory structural behavior of 304 stainless steel welded pressure vessels. Other nondestructive inspection techniques such as x-ray and dye penetrant are required in conjunction with a proof test. Furthermore, periodic proof tests were found to be detrimental since they caused a reduction in cyclic life relative to specimens that were subjected to only a single proof test at the start of the test.

## Recommendations

1. Since the reduction in cyclic life resulting from the application of periodic overloads may have been due to the high stress levels used during the overload, i.e., 95% of the yield stress, additional cyclic tests should be conducted using stress levels representative of membrane stresses in full scale vessels. Tests both with and without an initial proof overload are required to evaluate the effect of proof tests that are normally required by fabrication and testing specifications.

2. Tests should be undertaken to evaluate the effect of both magnitude of the proof test factor and proof test frequency on cyclic life of 304 stainless steel weldments. These tests would form a basis for selecting the optimum combination of proof factor and frequency for cryogenic pressure vessels.

## REFERENCES


1. C. F. Tiffany, "Fracture Control of Metallic Pressure Vessels," NASA Space Vehicle Design Criteria (Structures) NASA SP-8040, May 1970

2. H. H. Johnson and P. C. Paris, "Subcritical Flaw Growth," Engineering Fracture Mechanics, Vol. 1, No. 1, June 1968

3. W. F. Brown, Jr. and J. E. Srawley, "Plane Strain Crack Toughness Testing of High Strength Metallic Materials," ASTM STP 410, December 1967

4. R. C. Shah and A. S. Kobayashi, "On the Surface Flaw Problem," The Surface Crack: Physical Problems and Computational Solutions, ASME Publication, October 1972

5. American Iron and Steel Institute, "Type 304 and 304L Stainless and Heat Resisting Steels," June 1957

6. E. S. Folias, "An Axial Crack in a Pressurized Cylindrical Shell," Int. Journ. Fract. Mech., Vol. 1, No. 2, 1965

7. G. G. Hancock and H. H. Johnson, "Subcritical Crack Growth in AM350 Steel," Materials Research and Standards, 6, 1966

8. C. F. Tiffany, P. M. Lorenz, and L. R. Hall, "Investigation of Plane Strain Flaw Growth in Thick-Walled Tanks," NASA CR-54837, February 1966

## APPENDIX - CONVERSION OF U.S. CUSTOMARY UNITS TO SI UNITS

In the text of this report, all numerical values are given in U.S. customary units with corresponding SI units in parentheses. Due to the complexity of the tables of results, only U.S. customary units are used therein. Conversion factors for converting U.S. customary to SI units are given in the following table:

| To Convert From (U.S. Customary Units) | Multiply by | To Obtain (SI Units) |
|---|---|---|
| in. | $2.54 \times 10^{-2}$ | meter (m) |
| lbf | 4.448 | newton (n) |
| kip | 4.448 | kilonewton (kN) |
| ksi | 6.895 | meganewton/meter$^2$ ($MN/m^2$) |
| ksi $\sqrt{\text{in}}$ | 1.099 | $MN/m^{3/2}$ |
| °F | 5/9 (F + 459.67) | °K |

*Table 1: Test Program For 304 Stainless Steel Annealed Base Metal and As-Welded Welds*

| TYPE OF TEST | CRACK | | TEST TEMP ($^{O}$F) /ENV | NUMBER OF TESTS |
|---|---|---|---|---|
| | TYPE | LOCATION | | |
| FRACTURE RESISTANCE SURVEY | CENTER CRACK | WELD $\mathcal{C}_L$ | 72/AIR | 1 |
| | | WELD FL | | 1 |
| | | WELD HAZ | | 1 |
| | | BASE METAL | | 1 |
| | | WELD $\mathcal{C}_L$ | -320/$LN_2$ | 2 |
| | | WELD $\mathcal{C}_L$ | -423/$LH_2$ | 2 |
| | SURFACE FLAW | WELD $\mathcal{C}_L$ | 72/AIR | 1 |
| | | WELD FL | | 1 |
| | | WELD HAZ | | 1 |
| | | BASE METAL | | 1 |
| LOAD–UNLOAD | SURFACE FLAW | WELD $\mathcal{C}_L$ | 72/AIR | 4 |
| | | | -320/$LN_2$ | 4 |
| | | | -423/$LH_2$ | 4 |
| SUSTAINED LOAD | SURFACE FLAW | WELD $\mathcal{C}_L$ | 60/$GH_2$ | 4 |
| | | | -320/$LN_2$ | 2 |
| | | | -423/$LH_2$ | 2 |
| CYCLIC LOAD | SURFACE FLAW | WELD $\mathcal{C}_L$ | 72/AIR | 4 |
| | | | -320/$LN_2$ | 4 |
| | | | -423/$LH_2$ | 4 |
| PROGRAMMED CYCLIC LOAD | SURFACE FLAW | WELD $\mathcal{C}_L$ | 72/AIR (-320/$LN_2$)[a] | 1 2 |

(a) OVERLOAD CYCLE AT 72$^{O}$F (AIR), SUBSEQUENT CYCLES AT -320/$LN_2$

*Table 2: Specification Limits on Chemical Composition For AISI 304 Stainless Steel Plate and AISI 308 Stainless Steel Weld Wire*

| MATERIAL | LIMIT | ELEMENT (% BY WEIGHT) | | | | | | | | | |
|---|---|---|---|---|---|---|---|---|---|---|---|
| | | Cr | Ni | C | Cu | Si | Mn | P | S | Mo | Fe |
| AISI 304 STAINLESS STEEL PLATE | MAX | 20.0 | 12.0 | 0.08 | 0.50 | 1.00 | 2.00 | 0.045 | 0.030 | 0.50 | Bal |
| | MIN | 18.0 | 8.0 | – | – | – | – | – | – | – | Bal |
| AISI 308 STAINLESS STEEL WELD WIRE | MAX | – | 12.0 | 0.07 | – | 1.00 | 2.00 | 0.030 | 0.030 | – | Bal |
| | MIN | 20.0 | 9.5 | – | – | – | – | – | – | – | Bal |

*Table 3: Mechanical Property Test Results for 304 Stainless Steel Base and Weld Metal*

| MATERIAL | | SPECIMEN | | | TEST | | PROPERTIES | | | |
|---|---|---|---|---|---|---|---|---|---|---|
| CONDITION | GRAIN DIRECTION | NUMBER | GAGE THICKNESS (IN.) | GAGE WIDTH (IN.) | ENVIRONMENT | TEMPERATURE ($^{o}$F) | ULTIMATE TENSILE STRENGTH (KSI) | 0.2% OFFSET YIELD STRENGTH (KSI) | REDUCTION IN AREA (%) | ELONGATION IN 2.0-INCH GAGE LENGTH (%) |
| BASE METAL | L* | SL-1 | 0.352 | 0.500 | AIR | 72 | 88.9 | 47.6 | 73 | 64 |
| | L | SL-2 | 0.352 | 0.500 | AIR | 72 | 88.8 | 47.6 | 74 | 64 |
| | T* | ST-1 | 0.352 | 0.500 | AIR | 72 | 87.7 | – | 78 | 66 |
| | T | ST-2 | 0.352 | 0.500 | AIR | 72 | 88.6 | 46.1 | 77 | 67 |
| | L | SL-3 | 0.252 | 0.501 | $LN_2$ | -320 | 229.9 | 54.7 | 49 | 39 |
| | T | ST-4 | 0.251 | 0.498 | $LN_2$ | -320 | 234.8 | 58.1 | 55 | 42 |
| | L | SL-4 | 0.253 | 0.500 | $LH_2$ | -423 | 244.1 | 59.4 | – | – |
| | T | ST-3 | 0.236 | 0.506 | $LH_2$ | -423 | 215.0 | 52.8 | – | – |
| WELD METAL | WELD ∥ TO L DIRECTION | SWT-1 | 0.353 | 0.504 | AIR | 72 | 83.7 | 46.2 | 42 | 31 |
| | | SWT-2 | 0.358 | 0.504 | AIR | 72 | 84.6 | 51.3 | 36 | 31 |
| | | SWT-3 | 0.254 | 0.507 | $LN_2$ | -320 | 107.2 | 58.6 | 12 | 11 |
| | | SWT-4 | 0.253 | 0.487 | $LN_2$ | -320 | 133.3 | 57.1 | 15 | 16 |
| | | SWT-5 | 0.252 | 0.507 | $LH_2$ | -423 | 116.2 | 70.0 | – | – |
| | | SWT-6 | 0.253 | 0.505 | $LH_2$ | -423 | 130.9 | 65.5 | – | – |

* L = Longitudinal

T = Long Transverse

∥ = Parallel

*Table 4: Results For Fracture Resistance Survey Tests Of 304 Stainless Steel Weldments In 72$^{0}$ F Air*

| SPECIMEN | | | SURFACE FLAW | | | APPLIED GROSS STRESS | |
|---|---|---|---|---|---|---|---|
| NUMBER | THICKNESS (IN.) | WIDTH (IN.) | LOCATION | DEPTH 'a' (IN.) | LENGTH '2c' (IN.) | AT FLAW BREAKTHRU (KSI) | AT FAILURE (KSI) |
| 10-1 | 0.391 | 7.501 | B.M | 0.261 | 1.80 | 55.6 | 55.6 |
| 10-3 | 0.387 | 7.502 | F.L * | 0.264 | 1.81 | 52.9 | 53.4 |
| 10-5 | 0.393 | 7.510 | F.L * | 0.261 | 1.80 | 55.9 | 56.5 |
| 5-1 | 0.388 | 7.501 | WELD $\mathbb{C}_L$ | 0.276 | 1.77 | 53.1 | 55.1 |

* ACTUALLY LOCATED IN WELD METAL ADJACENT TO FUSION LINE

*Table 5: Results For Tests of 304 Stainless Steel Center Cracked Panels*

| SPECIMEN DETAILS | | | TEST CONDITIONS | | | CRACK DETAILS | | | MINIMUM CRITICAL CRACK LENGTH IN FULL SCALE DEWARS AT | |
|---|---|---|---|---|---|---|---|---|---|---|
| NUMBER | THICKNESS (IN.) | WIDTH (IN.) | MEDIUM | TEMPERATURE ($^{o}$F) | MAX GROSS SECTION STRESS (KSI) | LOCATION | INITIAL LENGTH (IN.) | FINAL LENGTH (IN.) | $\sigma$ = 47 KSI (GROSS) | $\sigma$ = 31 KSI (GROSS) |
| CC-3 | 0.372 | 23.78 | AIR | 72 | 24.8 | WELD $\mathbb{C}_L$ | 11.93 | 12.35 | 4.3 | 9.6 |
| CC-1 | 0.374 | 23.80 | | | 24.7 | F.L | 11.92 | 11.92 | 4.3 | 9.6 |
| CC-2 | 0.372 | 23.80 | | | 26.5 | HAZ | 11.97 | 11.97 | 4.9 | 11.1 |
| CC-5 | 0.399 | 23.80 | | | 24.7 | BM | 11.97 | 11.97 | 4.1 | 9.6 |
| CC-4 | 0.378 | 23.82 | $LN_2$ | -320 | 27.5 | WELD $\mathbb{C}_L$ | 12.12 | 12.12 | 4.4 | 9.9 |
| CC-6 | 0.386 | 23.78 | | | 27.5 | WELD $\mathbb{C}_L$ | 12.10 | 12.13 | 4.4 | 9.9 |
| CC-7 | 0.369 | 23.74 | $LH_2$ | -423 | 34.9 | WELD $\mathbb{C}_L$ | 12.00 | 12.35 | 5.0 | 11.3 |
| CC-8 | 0.392 | 23.81 | | | 34.7 | WELD $\mathbb{C}_L$ | 11.95 | * | 4.9 | 11.1 |

* NOT DETECTABLE. SPECIMEN FAILED AT INDICATED STRESS

NOTE: SEE SECTION 5.1 FOR DISCUSSION OF RESULTS

*Table 6: Load/Unload Test Results For 304 Stainless Steel Surface-Flawed Weld Centerlines*

| SPECIMEN | | | INITIAL FLAW | | TEST CONDITIONS | | | | FINAL FLAW | | |
|---|---|---|---|---|---|---|---|---|---|---|---|
| NUMBER | GAGE THICKNESS (IN.) | GAGE WIDTH (IN.) | DEPTH 'a' (IN.) | LENGTH '2c' (IN.) | MEDIUM | TEMPERATURE (°F) | PRESSURE (PSIG) | PEAK APPLIED STRESS (KSI) | DEPTH 'a' (IN.) | LENGTH '2c' (IN.) | FLAW DEPTH GROWTH, $\Delta a$ (IN.) |
| 9-3 | 0.388 | 7.005 | 0.075 | 0.45 | Air | 72 | 0 | 45 | 0.075 | 0.45 | 0 |
| 10-4 | 0.386 | 7.511 | 0.144 | 1.02 | | | | | 0.144 | 1.02 | 0 |
| 11-1 | 0.390 | 7.507 | 0.216 | 1.50 | | | | | 0.217 | 1.50 | 0.001 |
| 11-2 | 0.390 | 7.503 | 0.285 | 2.03 | | | | | 0.287 | 2.03 | 0.002 |
| 8-2 | 0.385 | 6.989 | 0.074 | 0.51 | $LN_2$ | -320 | 0 | 55 | 0.074 | 0.51 | 0 |
| 11-3 | 0.389 | 7.504 | 0.150 | 1.00 | | | | | 0.150 | 1.00 | 0 |
| 11-4 | 0.395 | 7.500 | 0.210 | 1.50 | | | | | 0.210 | 1.50 | 0.0005 |
| 11-5 | 0.383 | 7.508 | 0.280 | 2.00 | | | | | 0.281 | 2.00 | 0.0010 |
| 9-1 | 0.382 | 7.497 | 0.065 | 0.51 | $LH_2$ | -423 | 0 | 65 | 0.065 | 0.51 | 0 |
| 9-2 | 0.386 | 7.504 | 0.142 | 0.98 | | | | | 0.142 | 0.98 | 0 |
| 9-4 | 0.395 | 7.505 | 0.216 | 1.44 | | | | | 0.216 | 1.44 | 0 |
| 13-3 | 0.391 | 7.498 | 0.288 | 1.95 | | | | | 0.288 | 1.95 | 0 |

*Table 7: Sustained Load Test Results For 304 Stainless Steel Surface-Flawed Weld Centerlines*

| SPECIMEN | | | INITIAL FLAW | | TEST CONDITIONS | | | | | FINAL FLAW | | |
|---|---|---|---|---|---|---|---|---|---|---|---|---|
| NUMBER | GAGE THICKNESS (IN.) | GAGE WIDTH (IN.) | DEPTH 'a' (IN.) | LENGTH '2c' (IN.) | MEDIUM | TEMPERATURE (°F) | PRESSURE (PSIG) | APPLIED GROSS STRESS (KSI) | TEST DURATION (HOURS) | DEPTH 'a' (IN.) | LENGTH '2c' (IN.) | FLAW DEPTH GROWTH, $\Delta a$ (IN.) |
| 6-2 | 0.398 | 7.50 | 0.294 | 1.90 | $GH_2$ | 40-60 | 20 | 45.0 | 5.0 | 0.309 | 1.90 | 0.015 |
| 14-1 | 0.386 | 7.49 | 0.303 | 1.93 | | | | | 20.0 | 0.323 | 1.93 | 0.020 |
| 5-5 | 0.379 | 7.51 | 0.288 | 1.97 | | | | | 20.0 | 0.300 | 1.97 | 0.012 |
| 5-4 | 0.376 | 7.50 | 0.291 | 1.98 | Argon | 72 | 2-3 | 45.0 | 20.0 | 0.300 | 1.98 | 0.009 |
| 6-4 | 0.386 | 7.50 | 0.294 | 2.00 | $LN_2$ | -320 | 0 | 55.0 | 5.0 | 0.299 | 2.00 | 0.005 |
| 6-5 | 0.382 | 7.50 | 0.294 | 2.03 | | | | | 15.7 | 0.299 | 2.03 | 0.005 |
| 6-3 | 0.391 | 7.51 | 0.279 | 1.89 | $LH_2$ | -423 | 0 | 65.0 | 5.0 | 0.289 | 1.89 | 0.010 |
| 6-14 | 0.393 | 7.51 | 0.294 | 1.90 | | | | | 20.0 | 0.297 | 1.90 | 0.003 |

*Table 8: Cyclic Test Results For 304 Stainless Steel Surface-Flawed Weld Centerlines*

| SPECIMEN | | | INITIAL FLAW | | TEST CONDITIONS | | | | | FINAL FLAW | | EVALUATION (See Figure 16) | | |
|---|---|---|---|---|---|---|---|---|---|---|---|---|---|---|
| NUMBER | GAGE THICKNESS, t (IN.) | GAGE WIDTH (IN.) | DEPTH, $a_i$ (IN.) | LENGTH, $(2c)_i$ (IN.) | MEDIUM | TEMP ($^{o}$F) | PROOF STRESS (KSI) | MAX CYCLIC STRESS (KSI) | MIN CYCLIC STRESS (KSI) | DEPTH, $a_f$ (IN.) | LENGTH, $(2C)_f$ (IN.) | NUMBER OF LOADING CYCLES | $t-a_i$ (IN.) | $t-a_f$ (IN.) |
| 8-1 | 0.378 | 7.502 | 0.065 | 0.050 | AIR | 72 | 45.0 | 30 | 0 | 0.078 | 0.50 | 10,000 | 0.313 | 0.300 |
| 8-4 | 0.387 | 7.500 | 0.138 | 1.00 | | | | | | 0.154 | 1.00 | 10,000 | 0.249 | 0.233 |
| 12-1 | 0.384 | 7.501 | 0.210 | 1.50 | | | | | | 0.384 | 1.67 | 16,405 | 0.174 | 0 |
| 12-2 | 0.383 | 7.476 | 0.291 | 2.00 | | | | | | 0.383 | 2.05 | 7,325 | 0.092 | 0 |
| 8-3 | 0.388 | 7.504 | 0.068 | 0.50 | $LN_2$ | -320 | 55.0 | 37 | 0 | 0.068 | 0.50 | 10,000 | 0.320 | 0.320 |
| 8-5 | 0.386 | 7.504 | 0.147 | 0.99 | | | | | | 0.157 | 0.99 | 10,000 | 0.239 | 0.229 |
| 12-5 | 0.383 | 7.500 | 0.210 | 1.50 | | | | | | 0.383 | 1.50 | 15,000 | 0.173 | 0 |
| 13-1 | 0.390 | 7.502 | 0.283 | 1.93 | | | | | | 0.390 | 1.93 | 7,426 | 0.105 | 0 |
| 12-4 | 0.386 | 7.480 | 0.080 | 0.53 | $LH_2$ | -423 | 65.0 | 43 | 4 | 0.080 | 0.52 | 2,250 | 0.306 | 0.306 |
| 12-3 | 0.381 | 7.504 | 0.141 | 1.02 | | | | | | 0.150 | 1.02 | 2,250 | 0.240 | 0.231 |
| 5-3 | 0.393 | 7.510 | 0.237 | 1.44 | | | | | | 0.265 | 1.44 | 2,250 | 0.156 | 0.128 |
| 5-2 | 0.359 | 7.505 | 0.291 | 1.92 | | | | | | 0.359 | 1.92 | 1,972 | 0.068 | 0 |
| 14-5 | 0.356 | 7.490 | 0.273 | 1.91 | | | | | | 0.256 | 2.02 | 2,250 | 0.083 | 0 |

*Table 9: Programmed Load Cyclic Test Results For 304 Stainless Steel Surface-Flawed Weld Centerlines*

| SPECIMEN | | | INITIAL FLAW | | LOADING CONDITIONS [a] | | | | | RESULTS | | | | |
|---|---|---|---|---|---|---|---|---|---|---|---|---|---|---|
| | | | | | OVERLOADS | | BASELINE CYCLES | | | FLAW DIMENSIONS AT BREAKTHRU [b] | | | | |
| Number | Gage Thickness, Inch | Gage Width, Inch | Depth, $a_i$ Inch | Length, $(2c)_i$ Inch | Temperature °F | Peak Cyclic Stress, $\sigma_2$ KSI | Temperature, °F | Peak Cyclic Stress, $\sigma_1$ KSI | Test Medium | Depth, Inch | Length, Inch | Cycles to Crack Breakthru | Crack Length at Failure, Inch | Cycles to Failure |
| 7-2 | 0.359 | 7.50 | 0.280 | 2.03 | 72 | 45 | 72 | 30 | GHe | 0.359 | 2.03 | 2436 | 4.8 | 24,557 |
| 14-2 | 0.360 | 7.50 | 0.282 | 1.80 | 72 | 45 | -320 | 30 | GHe | 0.360 | 1.80 | 2263 | — | — |
| 14-4 | 0.363 | 7.50 | 0.260 | 1.84 | 72 | 45 | -320 | 30 | GHe | 0.363 | 1.84 | 3100 | — | — |

a Loading Conditions:

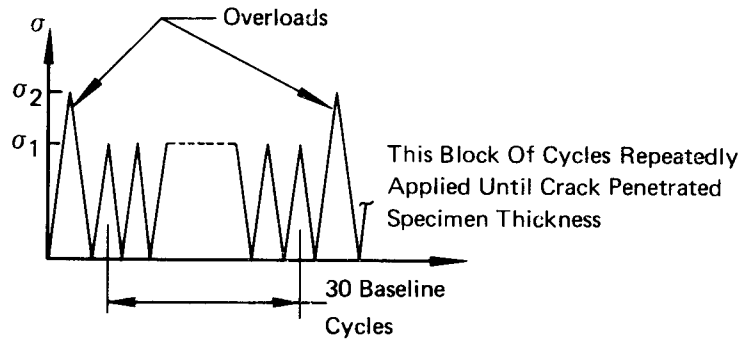


b Crack depth first penetrates specimen thickness

c Specimen cycled under uniform cyclic stress of 30 ksi after crack breakthru

*Table 10: Static Fracture Data For 304 Stainless Steel Surface Flawed Weld Centerlines In 72°F Air*

| SPECIMEN | | | FLAW | | |
|---|---|---|---|---|---|
| NUMBER | GAGE THICKNESS (IN.) | GAGE WIDTH (IN.) | DEPTH, a (IN.) | LENGTH, 2c (IN.) | FAILURE STRESS (KSI) |
| 5-3 | 0.393 | 7.51 | 0.232 | 1.43 | 60.3 |
| 9-4 | 0.395 | 7.50 | 0.325 | 1.47 | 54.5 |
| 6-3 | 0.391 | 7.51 | 0.369 | 1.92 | 51.4 |
| 14-3 | 0.393 | 7.51 | 0.381 | 1.94 | 51.4 |
| 6-2 | 0.398 | 7.51 | 0.386 | 1.94 | 50.2 |
| 13-1 | 0.390 | 7.50 | 0.390 | 1.94 | 51.3 |
| 5-4 | 0.376 | 7.50 | 0.376 | 2.08 | 49.4 |

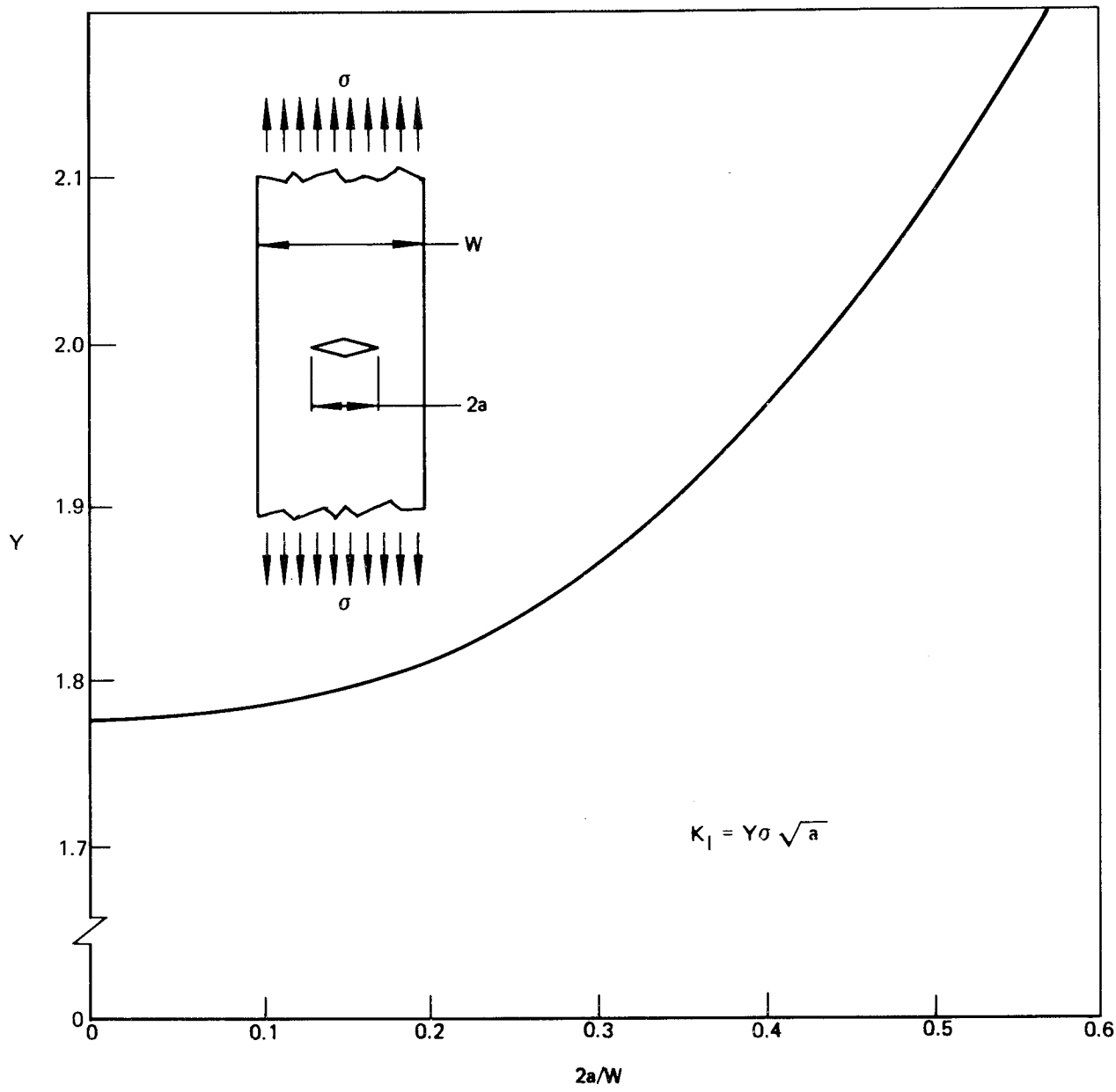


*Figure 1: Stress Intensity Factors for Center Cracked Specimens (Ref. 3)*

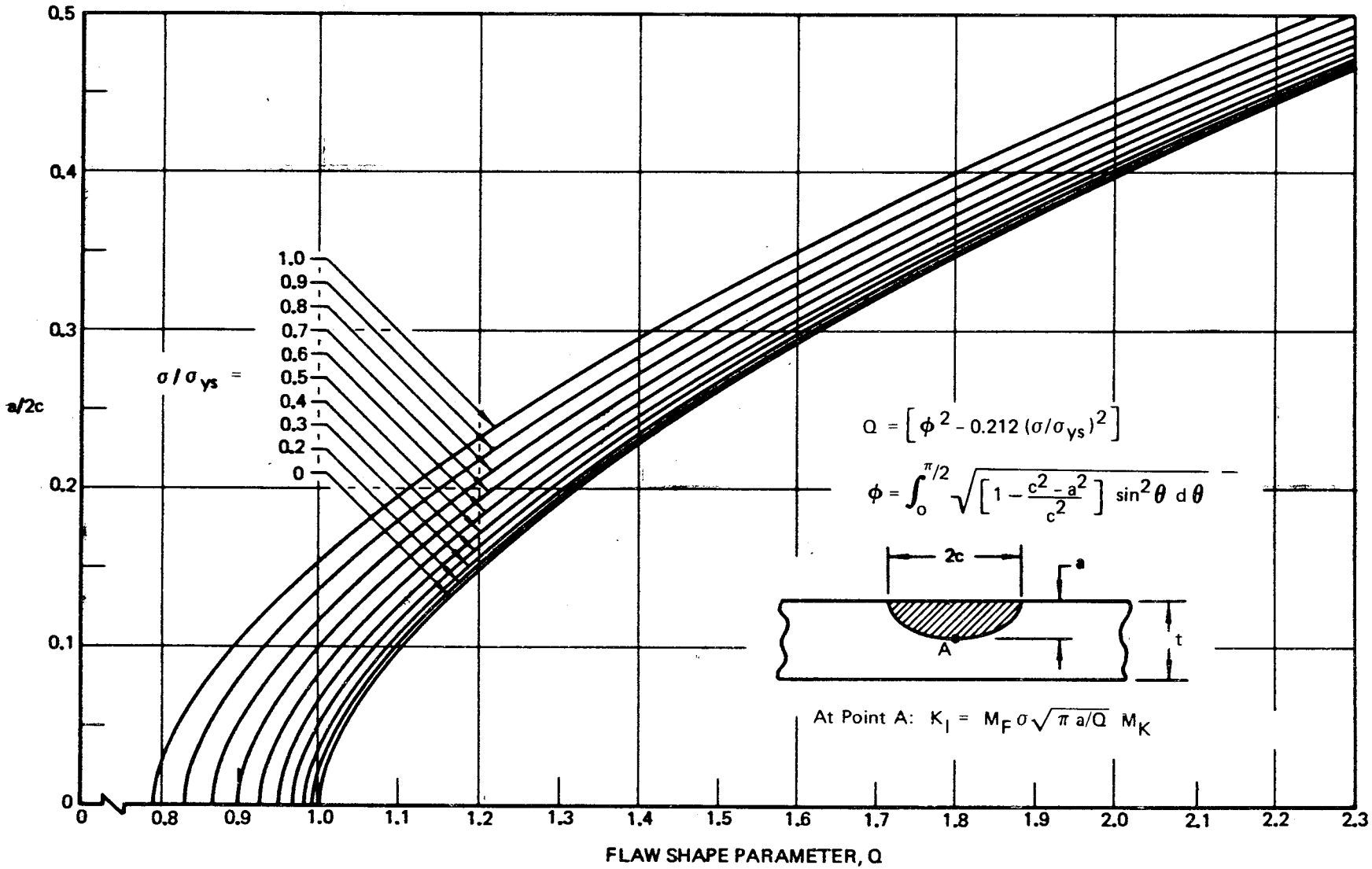


*Figure 2: Shape Parameter Curves for Surface Flaws*

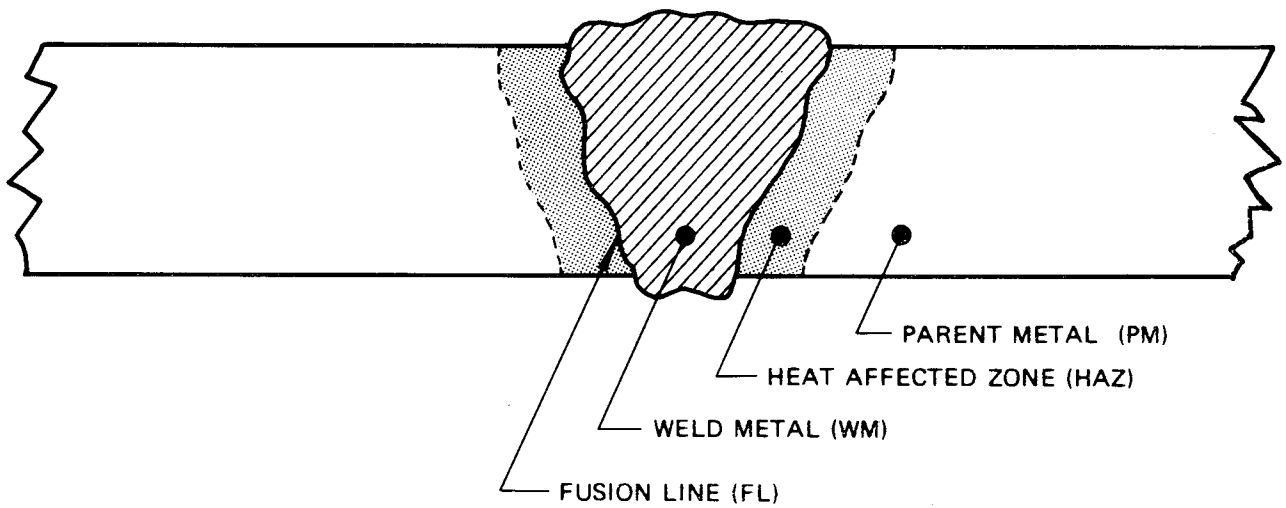


*Figure 3: Identification of Weldment Zones*

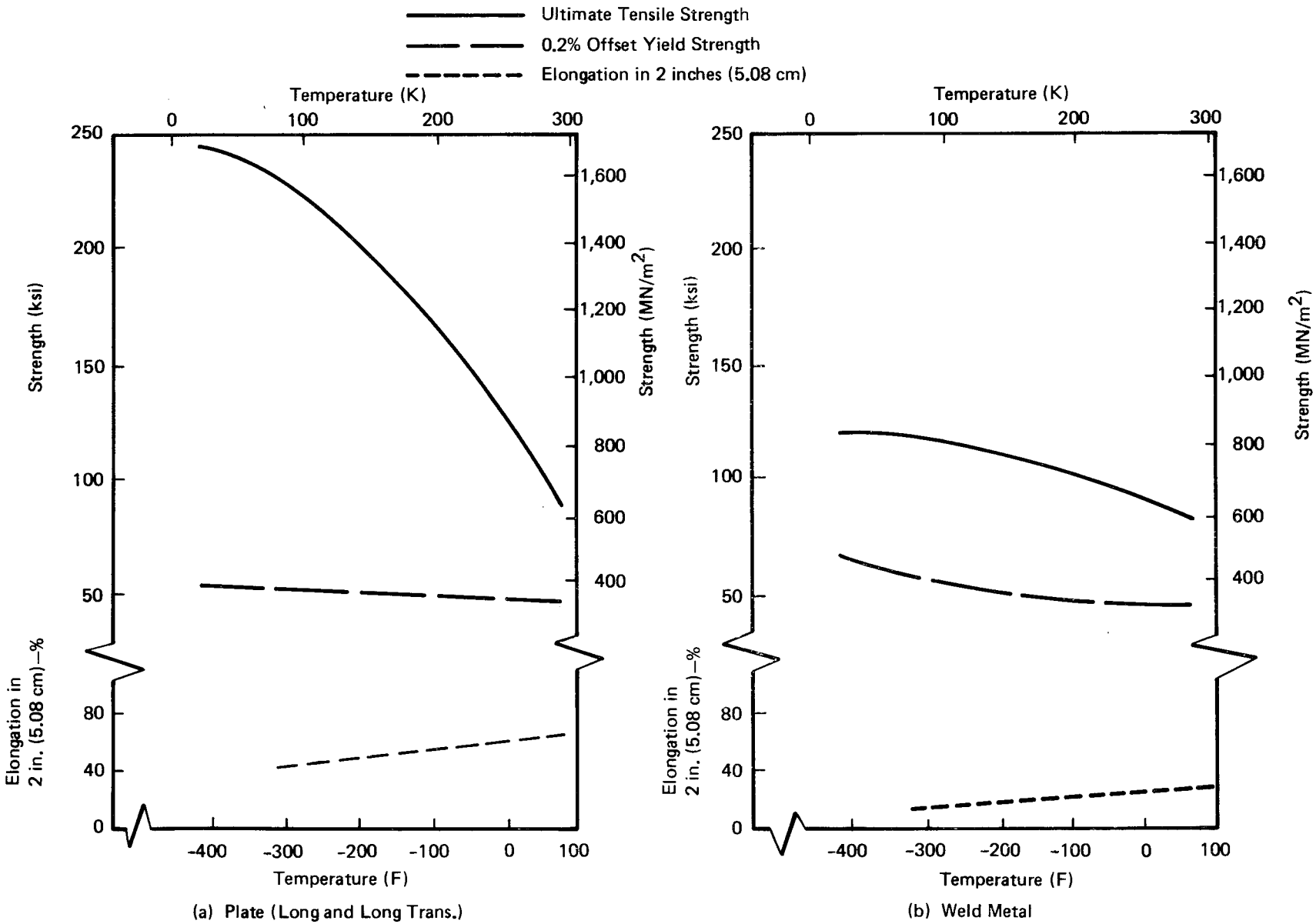


*Figure 4: Mechanical Properties for 304 Stainless Steel Plate and Weld Metal*

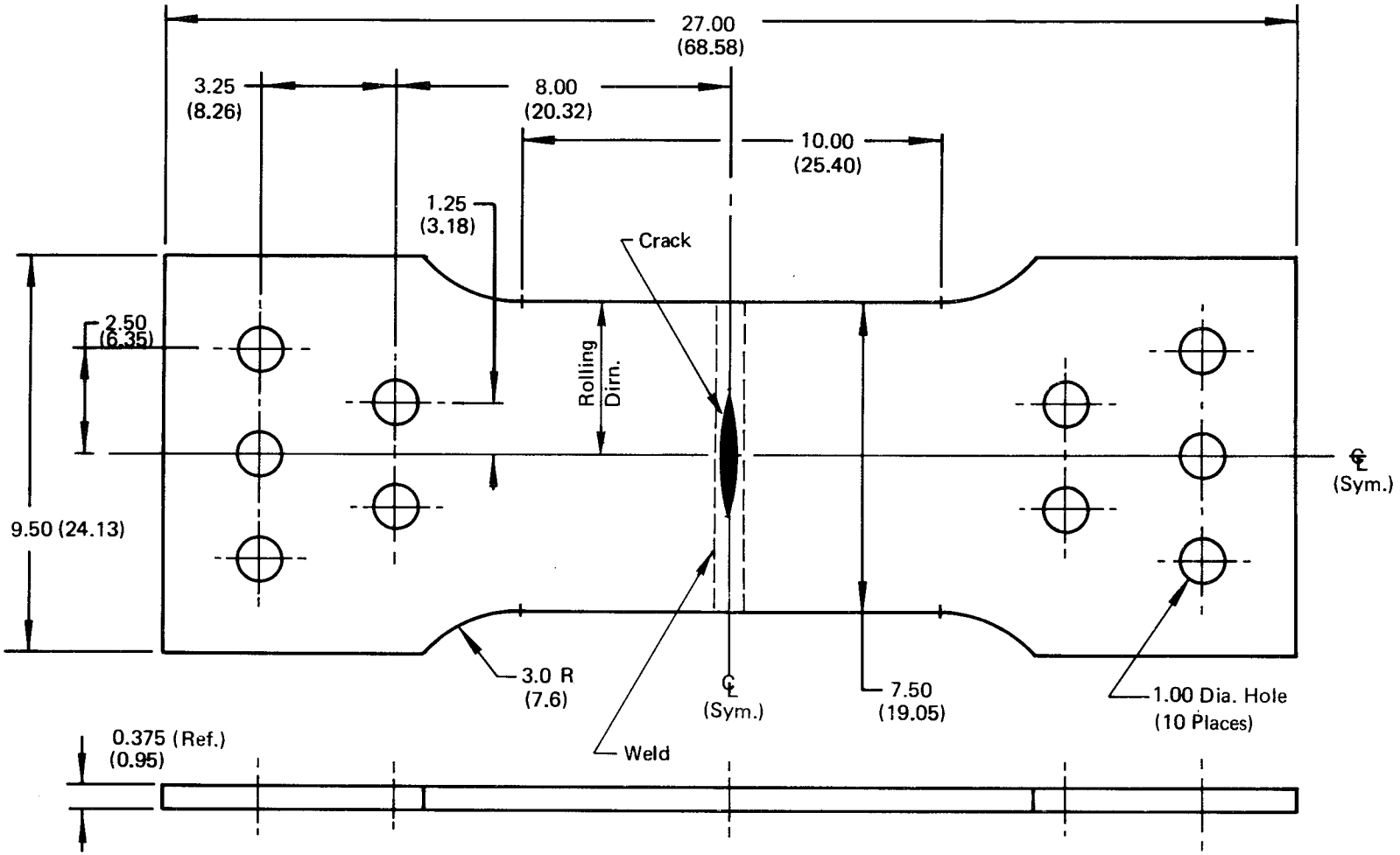


NOTE: All dimensions in inches (cm)

*Figure 5: 304 Stainless Steel Surface Flawed Specimen*

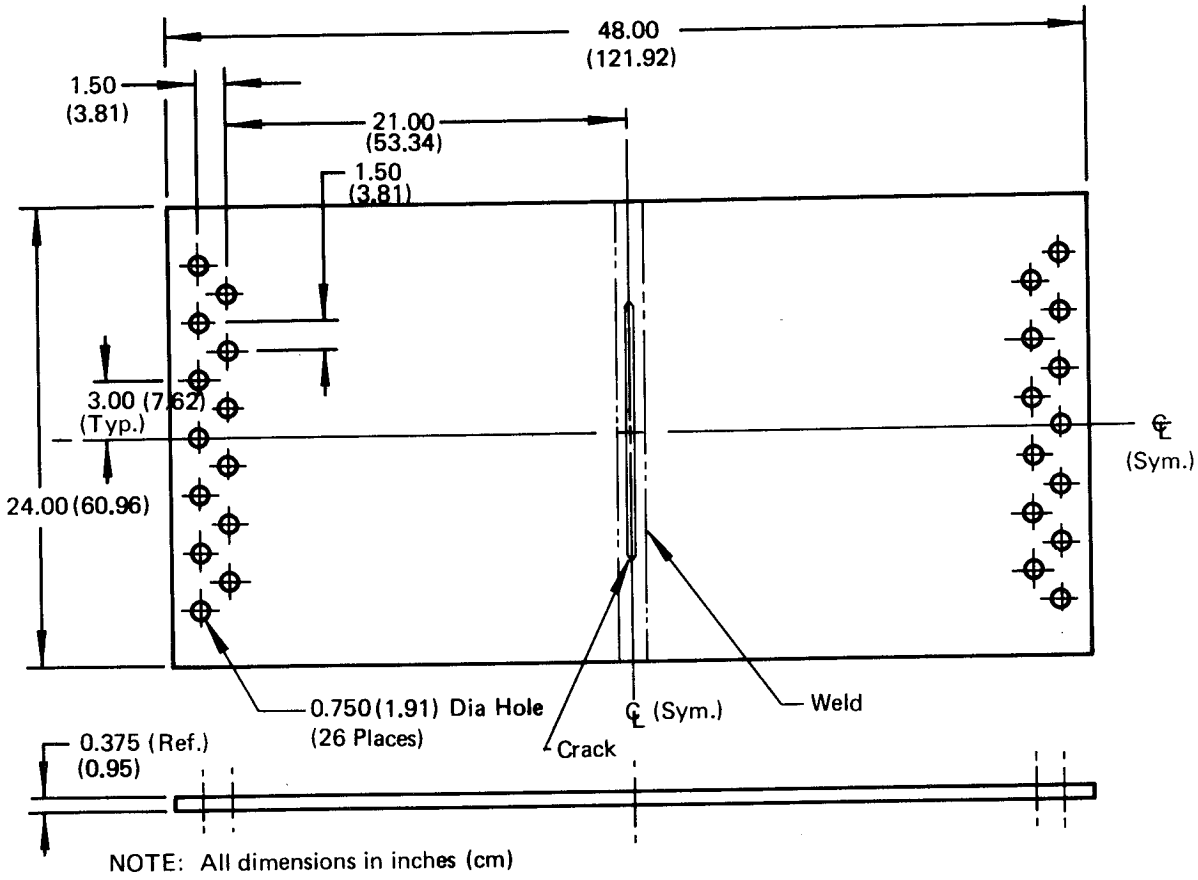


*Figure 6: 304 Stainless Steel Center Cracked Specimen*

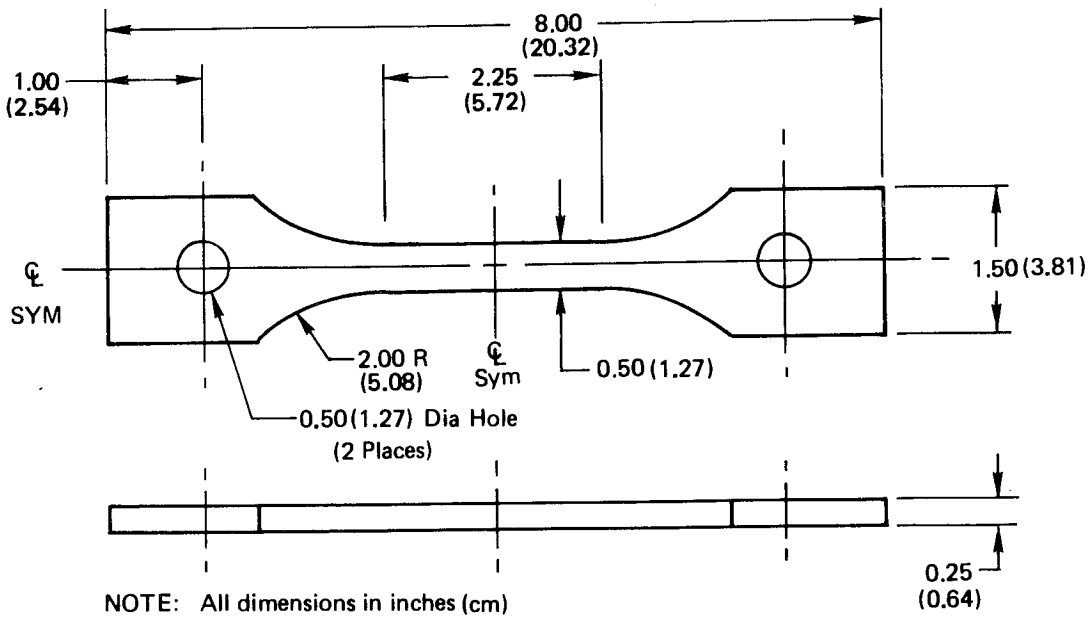


*Figure 7: Mechanical Property Test Specimen for 304 Stainless Steel*

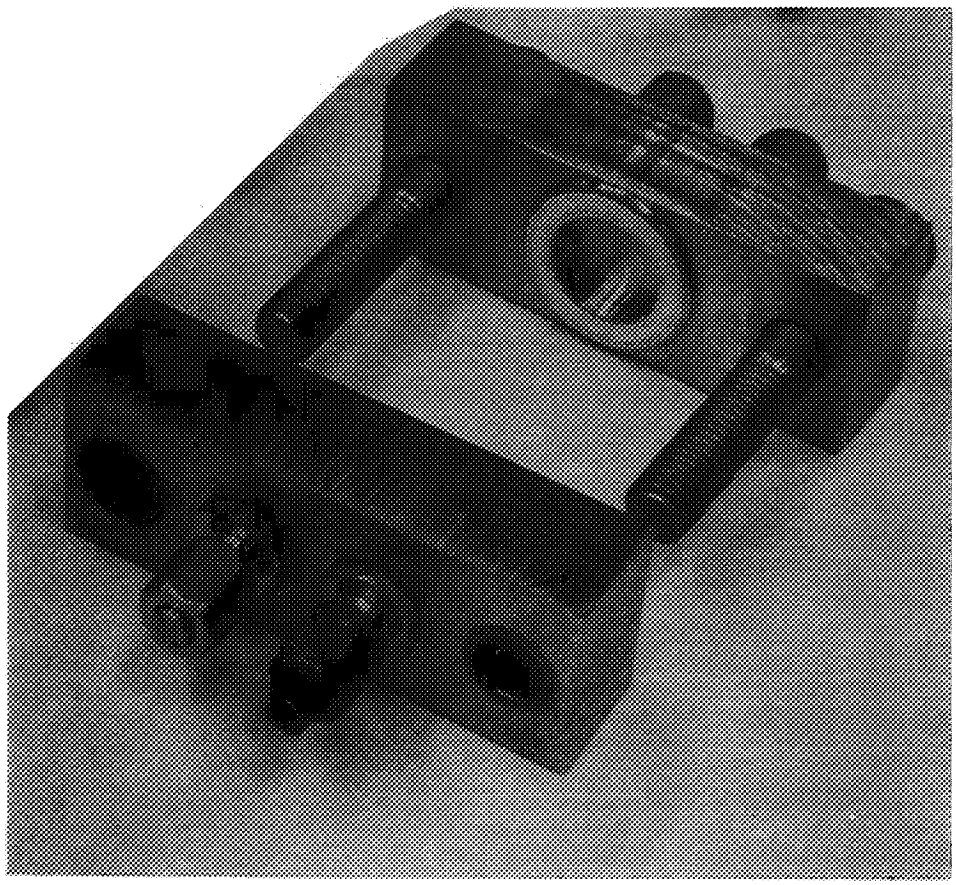

*Figure 8: Pressure Cups Used to Detect Crack Breakthrough in Surface Flawed Specimens*

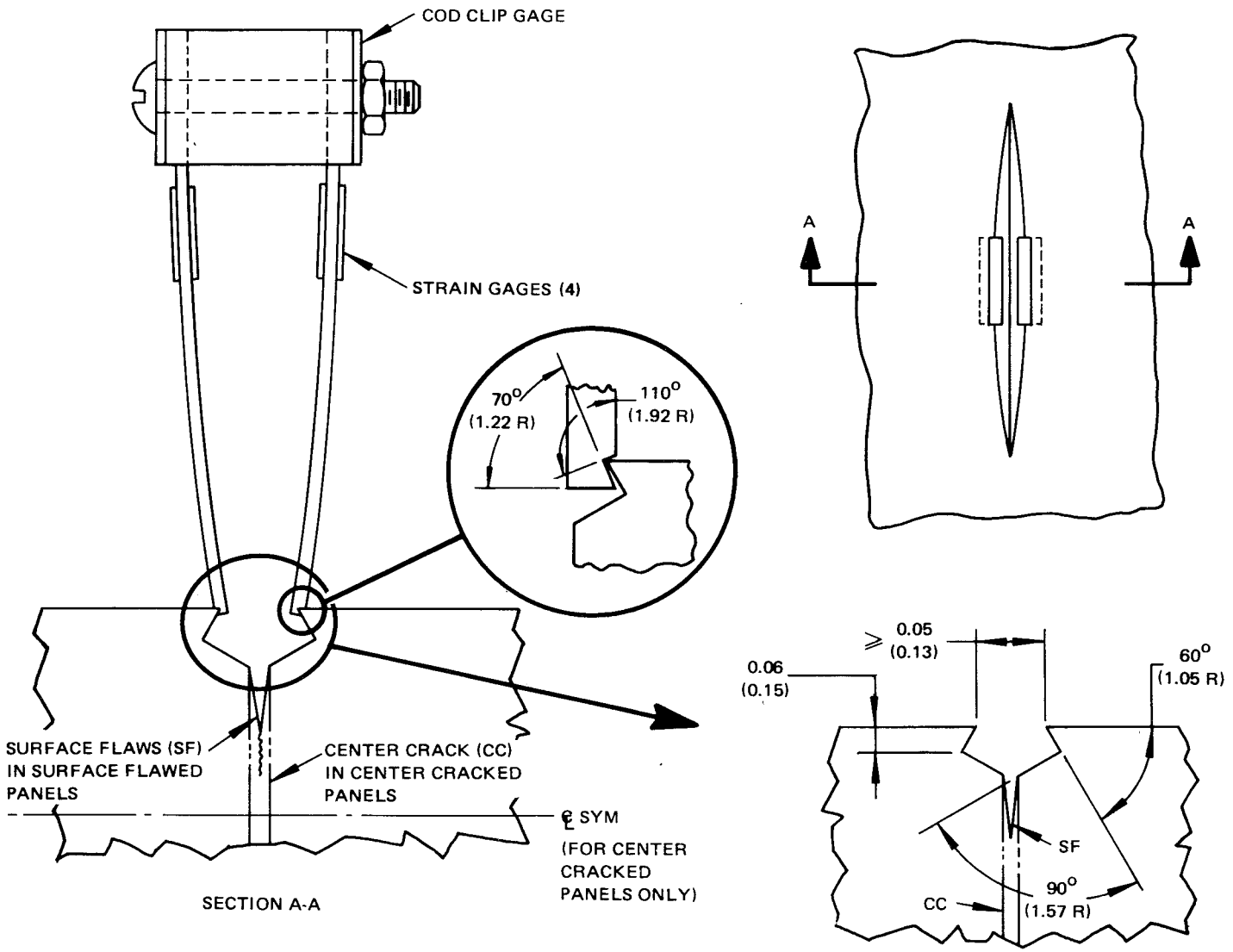


LINEAR DIMENSIONS GIVEN IN INCHES (CENTIMETERS)
AND ANGLES GIVEN IN DEGREES (RADIANS)

*Figure 9: Clip Gage Instrumentation for Measuring Crack Surface Displacements*

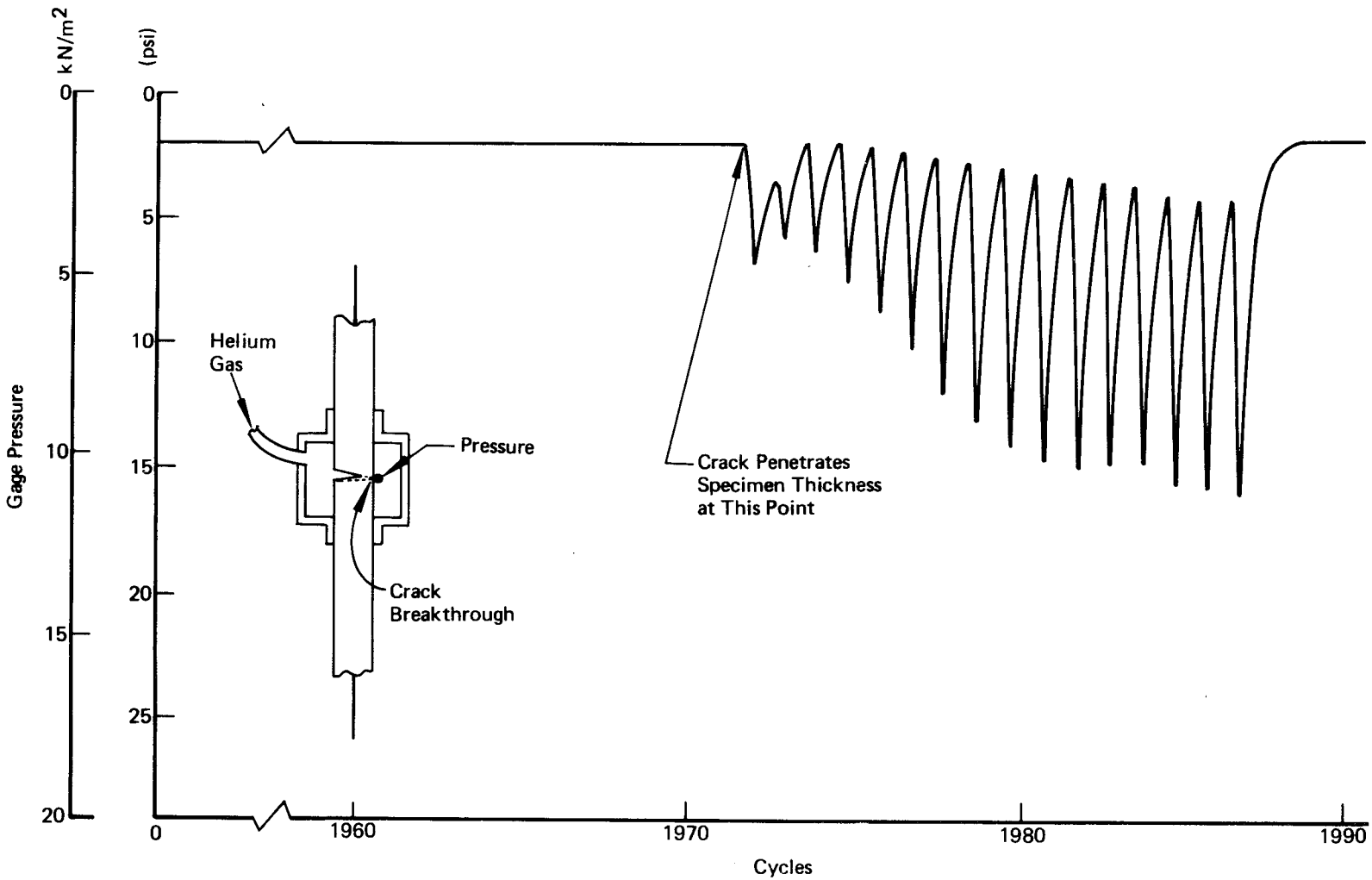


*Figure 10: Test Record Obtained From Instrumentation Used to Detect Crack Breakthrough In–423°F (20°K) Surface Flawed Tests*

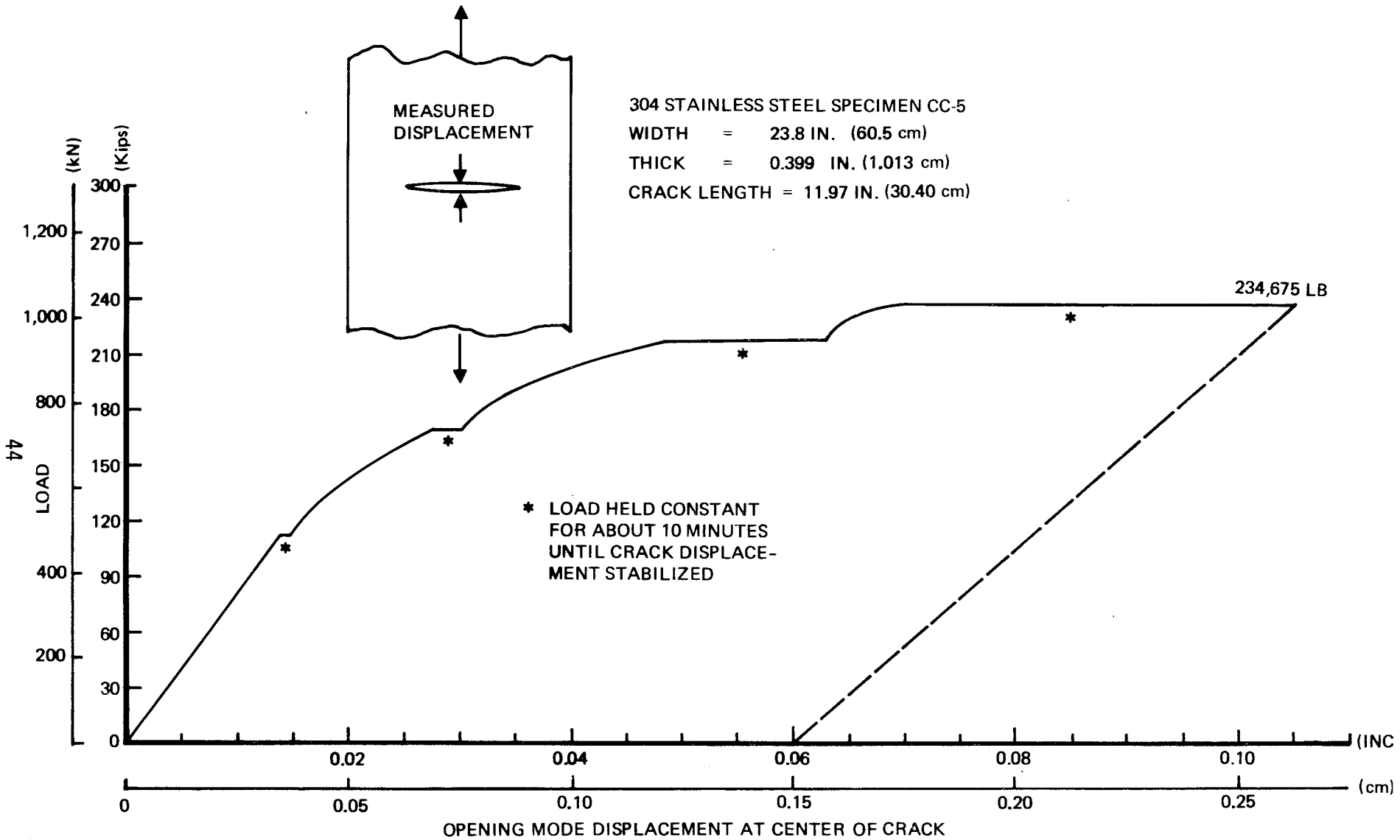


*Figure 11: Load Versus Crack Displacement Record for 304 Stainless Steel Center Cracked Specimen CC-5 Tested At 72°F (295K)*

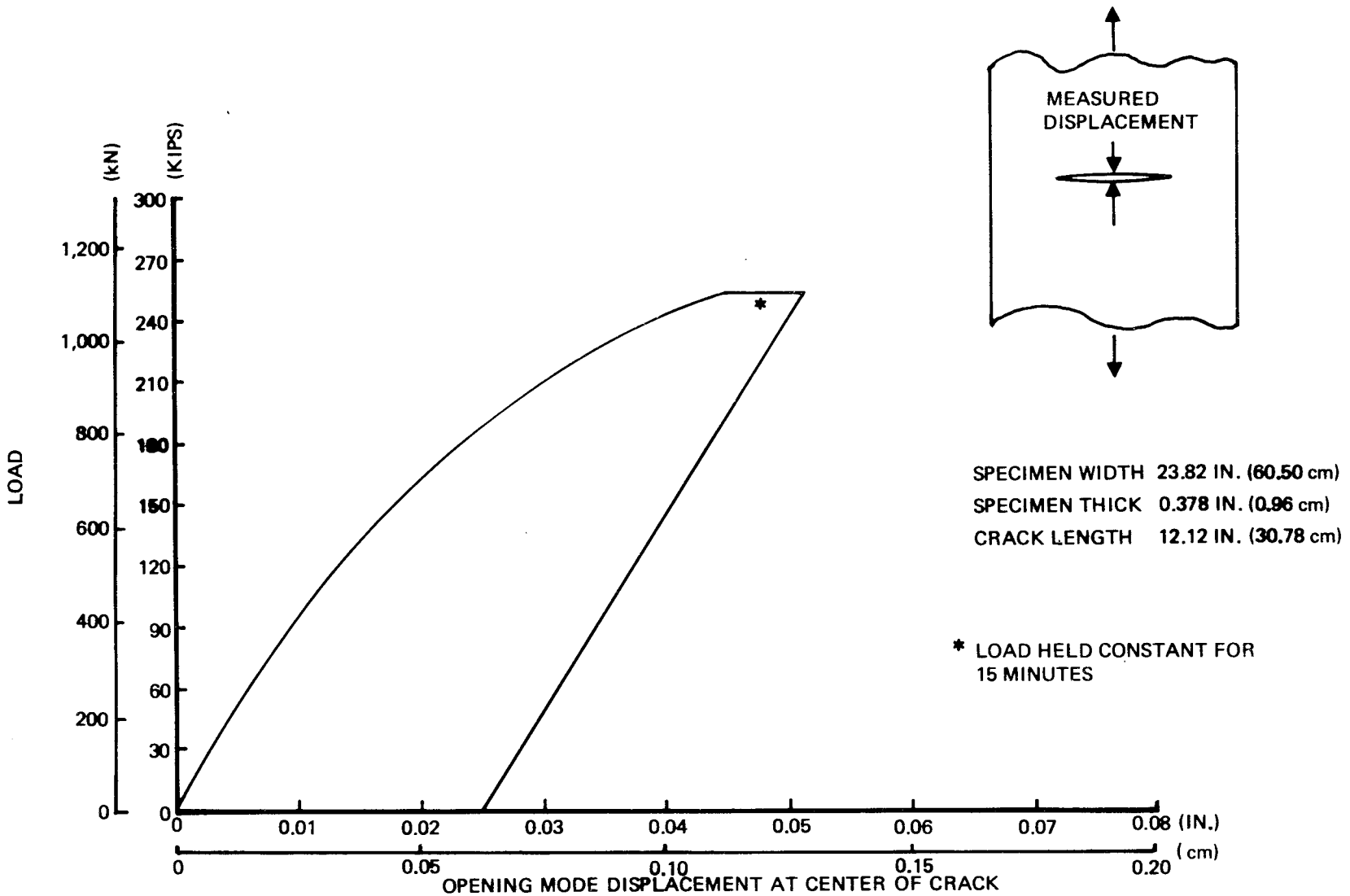


*Figure 12: Load Versus Crack Displacement Record for 304 Stainless Steel Center Cracked Specimen CC–4 Tested at –320° F (78 K)*

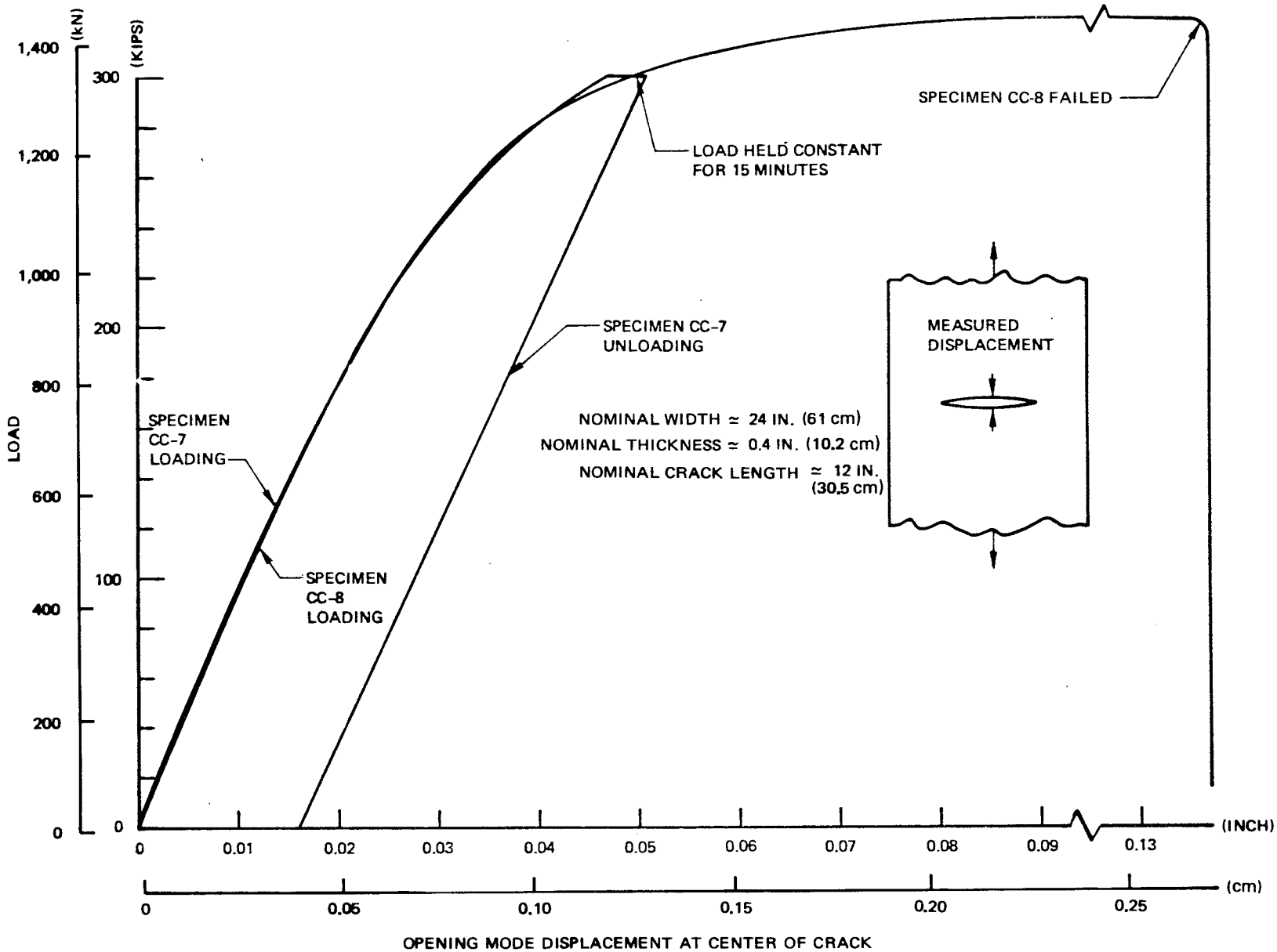


*Figure 13: Load Versus Crack Displacement Record For 304 Stainless Steel Center Cracked Specimens CC-7 & CC-8 Tested At -423F (20K)*

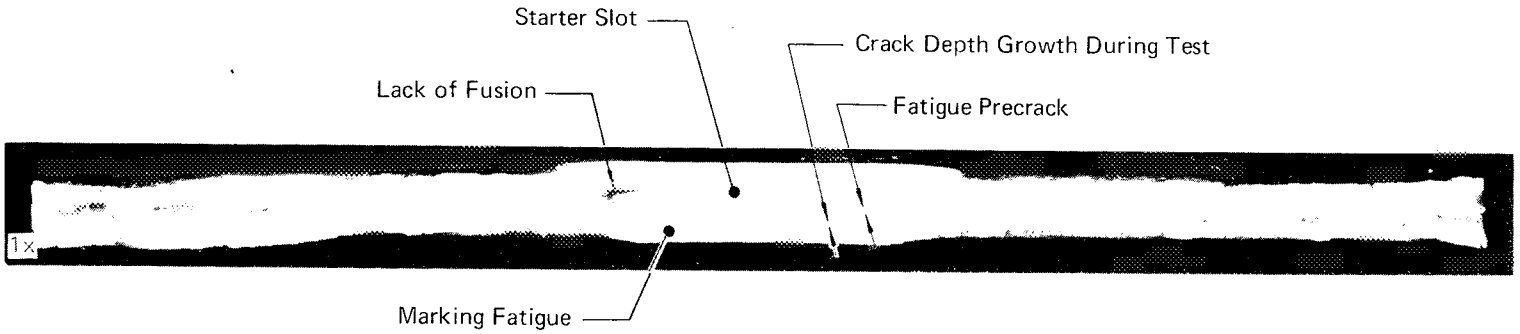


Sustained Load Specimen 14-1
Test Medium: $GH_2$ @ ~ 60°F (289 K)
Applied Stress: 45 ksi (310.3 $MN/m^2$)
Test Duration: 20 hrs.

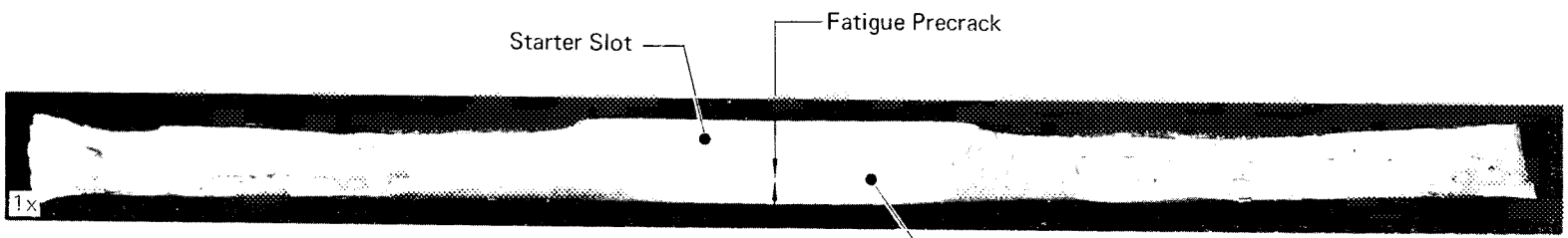


Cyclic Load Specimen 13-1
Test Medium: $LN_2$ @ -320°F (78 K)
Specimen Cycled Until Crack Barely
Penetrated Specimen Thickness
Applied Stress: 37 ksi (255.1 $MN/m^2$)
R = 0
N = 7436

*Figure 14: Fracture Surfaces of 304 Stainless Steel Surface Flawed Specimens 14-1 & 13-1*

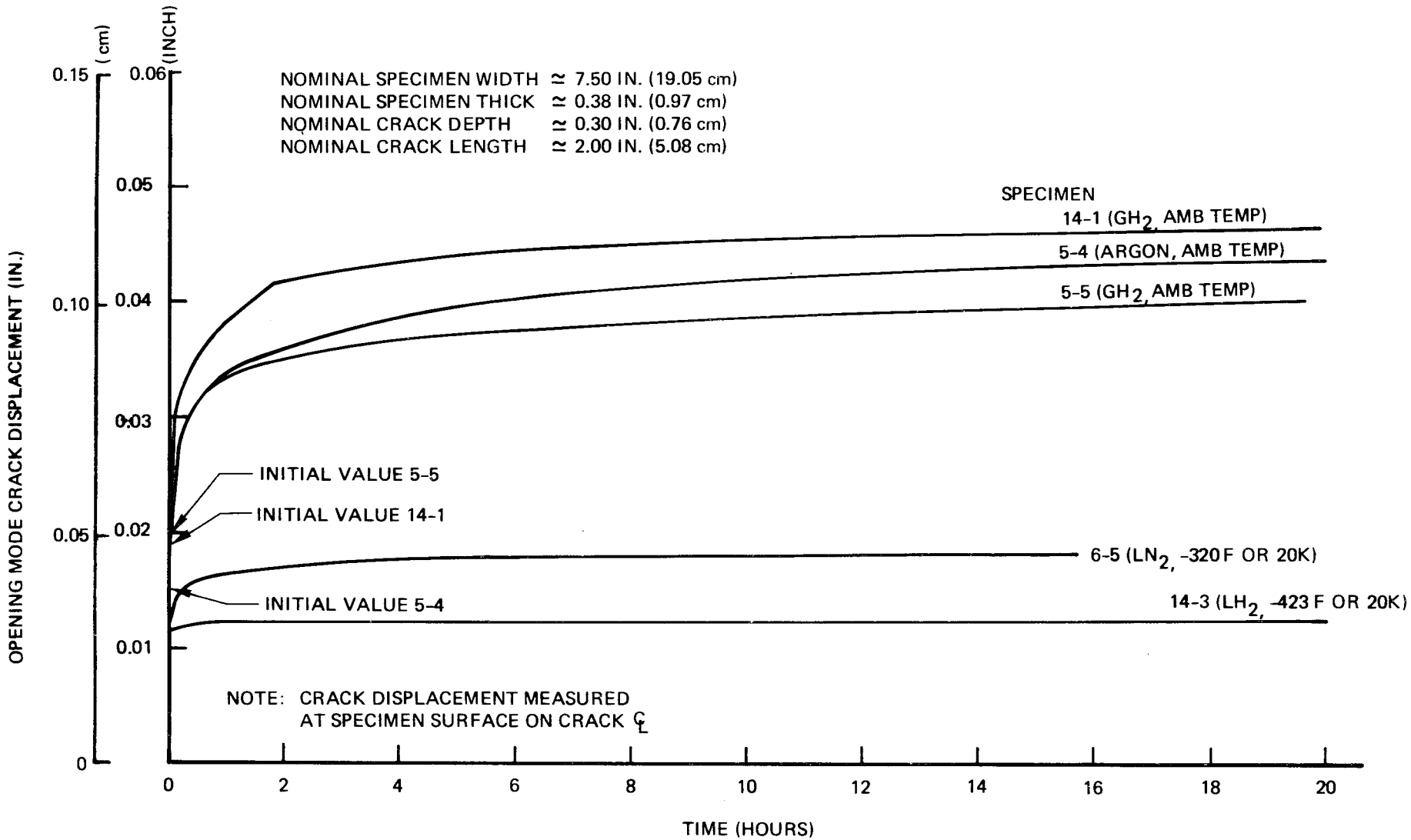


*Figure 15: Crack Displacement Vs Time Records For 304 Stainless Steel Surface Flawed Specimens*

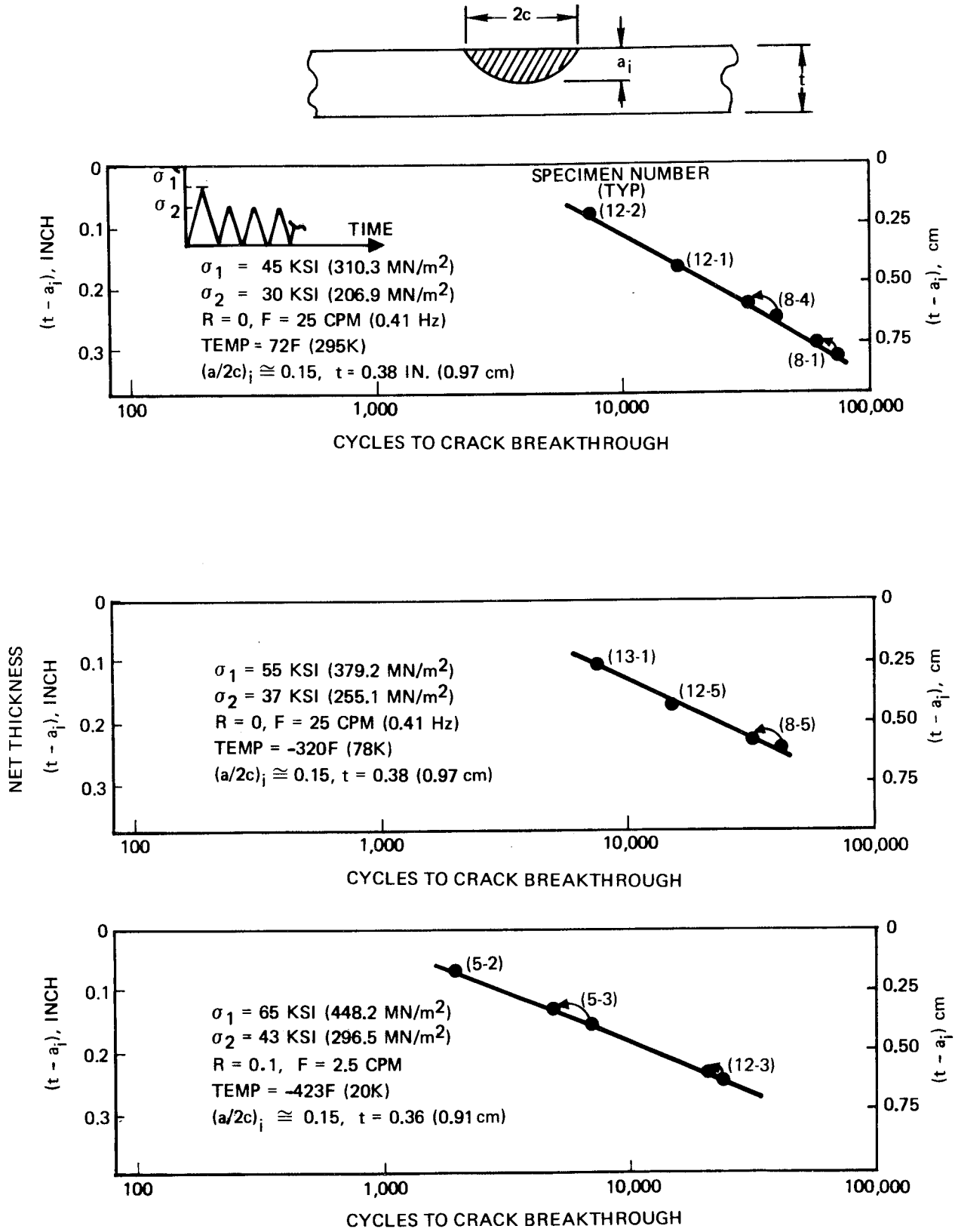


*Figure 16: Fatigue Crack Growth Data for 304 Stainless Steel Surface-Flawed Weld Centerlines*

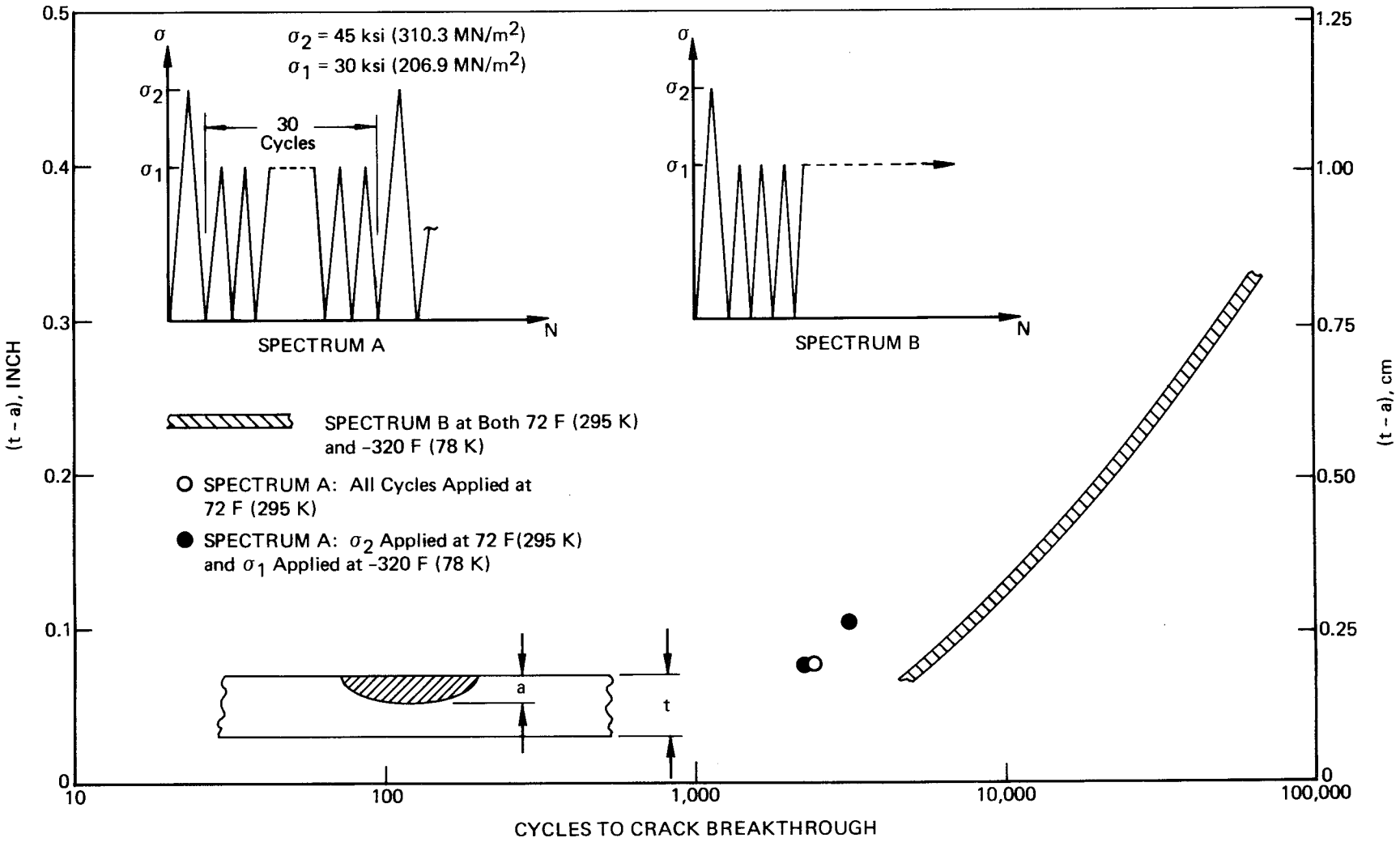


*Figure 17: Programmed Cyclic Load Test Results For 304 Stainless Steel Weld Centerlines*

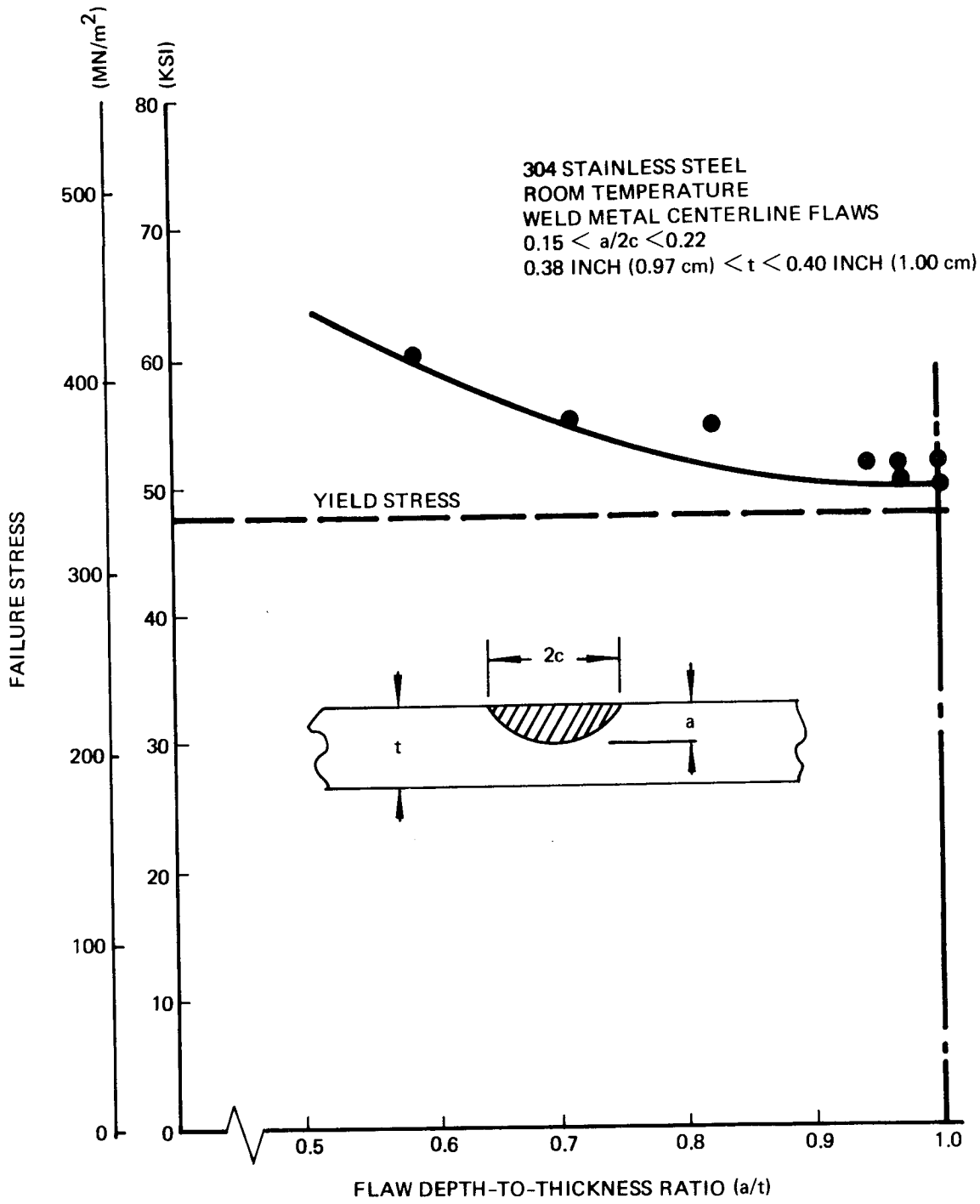


*Figure 18: Fracture Data For Surface Flawed 304 Stainless Steel Weld Centerlines*